

1 **High number concentrations of transparent exopolymer particles (TEP) in**
2 **ambient aerosol particles and cloud water – A case study at the tropical**
3 **Atlantic Ocean**

4
5 **Manuela van Pinxteren¹, Tiera-Brandy Robinson², Sebastian Zeppenfeld¹, Xianda Gong³⁺,**
6 **Enno Bahlmann⁴, Khanneh Wadinga Fomba¹, Nadja Triesch¹, Frank Stratmann³, Oliver Wurl²,**
7 **Anja Engel⁵, Heike Wex³, Hartmut Herrmann^{1*}**

8
9 *Corresponding author: Hartmut Herrmann (herrmann@tropos.de)

10
11 ¹ Atmospheric Chemistry Department (ACD), Leibniz-Institute for Tropospheric Research
12 (TROPOS), 04318 Leipzig, Germany

13 ² Institute for Chemistry and Biology of the Marine Environment, Carl-von-Ossietzky
14 University Oldenburg, 26382 Wilhelmshaven, Germany

15 ³ Dept. of Experimental Cloud and Microphysics, Leibniz-Institute for Tropospheric Research
16 (TROPOS), 04318 Leipzig, Germany

17 + now at: Center for Aerosol Science and Engineering, Department of Energy, Environmental
18 and Chemical Engineering, Washington University in St. Louis, 63130, MO, USA

19 ⁴ Leibniz Centre for Tropical Marine Research (ZMT), 28359 Bremen, Germany

20 ⁵ GEOMAR Helmholtz Centre for Ocean Research, Kiel 24105, Germany

34 Abstract

35 Transparent exopolymer particles (TEP) exhibit the properties of gels and are ubiquitously
36 found in the world oceans. Possibly, TEP may enter the atmosphere as part of sea spray
37 aerosol. Here, we report number concentrations of TEP with a diameter > 4.5 μm , hence
38 covering a part of the supermicron particle range, in ambient aerosol and cloud water samples
39 from the tropical Atlantic Ocean as well as in generated aerosol particles using a plunging
40 waterfall tank that was filled with the ambient seawater. The ambient TEP concentrations
41 ranged between 7×10^2 and 3×10^4 #TEP m^{-3} in supermicron aerosol particles and
42 correlations to sodium (Na^+) and calcium (Ca^{2+}) ($R^2 = 0.5$) suggested some contribution via
43 bubble bursting. Cloud water TEP concentrations were between 4×10^6 and 9×10^6 #TEP L^{-1} and,
44 according to the measured cloud liquid water content, corresponding to equivalent air
45 concentrations of $2 - 4 \times 10^3$ #TEP m^{-3} . ~~The TEP concentrations in the tank generated aerosol~~
46 ~~particles, produced from the same waters and sampled with an equivalent system, were~~
47 ~~significantly lower ($4 \times 10^2 - 2 \times 10^3$ #TEP m^{-3}) compared to the ambient concentrations.~~
48 Based on Na^+ concentrations in seawater and in the atmosphere, the enrichment factor for
49 TEP in the atmosphere was calculated. The tank-generated TEP were enriched by a factor of
50 50 compared to seawater and, therefore, in-line with published enrichment factors for
51 supermicron organic matter in general and TEP specifically. TEP enrichment in the ambient
52 atmosphere was on average 1×10^3 in cloud water and 9×10^3 in ambient aerosol particles and
53 therefore about two orders of magnitude higher than the corresponding enrichment from the
54 tank study. Such high enrichment of supermicron particulate organic constituents in the
55 atmosphere is uncommon and we propose that atmospheric TEP concentrations resulted
56 from a combination of enrichment during bubble bursting transfer from the ocean and a
57 secondary TEP in-situ formation in atmospheric phases. Abiotic in-situ formation might have
58 occurred from aqueous reactions of dissolved organic precursors that were present in particle
59 and cloud water samples, while biotic formation involves bacteria, which were abundant in
60 the cloud water samples.

61 The ambient TEP number concentrations were two orders of magnitude higher than recently
62 reported ice nucleating particle (INP) concentrations measured at the same location. As TEP
63 likely possess good properties to act as INP, in future experiments it is worth studying if a
64 certain part of TEP contributes a fraction of the biogenic INP population.

65

66 Keywords: Transparent exopolymer particles, marine aerosol particles, cloud water, plunging
67 waterfall tank, ice nucleating particles, Atlantic Ocean, Cape Verde Atmospheric Observatory
68 (CVAO)

69

70

71

72 1 Introduction

73 In marine ecosystems, polymer gels and gel-like material play an important role in the
74 biochemical cycling of organic matter (OM) (Passow, 2000, 2002b). One type of gel-like
75 particles, transparent exopolymer particles (TEP), have increasingly received attention. TEP
76 exist as individual particles rather than diffuse exopolymeric organic material and are
77 operationally defined as particles that are stained on 0.2 or 0.4 μm pore-sized polycarbonate
78 filters with the dye Alcian Blue (Passow, 2002b). TEP have shown surface-active properties
79 and are highly hydrated molecules (Passow et al. 2002a). Chemically, they consist of
80 polysaccharide chains including uronic acids or sulphated monosaccharides that are bridged
81 with divalent cations (mostly calcium) (Alldredge et al., 1993;Bittar et al., 2018).

82 In contrast to solid particles, TEP **have** properties of gels; with similar constituents
83 (carrageenans, alginic acid, and xanthan) to those that form gels, spontaneously forming from
84 dissolved fibrillar colloids, and they can be broken up by Calcium chelators such as EDTA.
85 However, because TEP have not yet been seen to undergo phase transition they can officially
86 only be classified as gel-like particles (Verdugo et al., 2004). Regardless though, TEP have been
87 shown to be highly important in sedimentation processes and carbon cycling in the sea (Mari
88 et al., 2017), as well as highly prevalent in the sea surface microlayer (SML) (Robinson et al.,
89 2019a) with a potentially significant effect on air-sea release of marine aerosols.

90 Generally, TEP can be formed via two pathways. First, the biotic pathway happens via
91 a breakdown and secretion of precursor material from an organism or via a direct release as
92 particles from aquatic organisms, e.g. as metabolic-excess waste products when nutrients are
93 limited (Decho and Gutierrez, 2017;Engel et al., 2004;Engel et al., 2002). High TEP
94 concentrations are usually associated with phytoplankton blooms, with the majority of
95 precursor material being released by diatoms and to a lesser extent other plankton species.
96 However, bacteria are also associated with TEP production, although their exact role is still
97 not resolved (Passow, 2002a). Secondly, TEP form through abiotic pathways. These could be
98 spontaneous formation from dissolved organic precursors (e.g. dissolved polysaccharides)
99 that are released by aquatic organisms. The abiotic formation is enhanced by turbulent or
100 laminar shear (Engel et al., 2002;Passow, 2000). Recent studies confirmed that higher wind
101 speeds, forming breaking waves, could be an effective transport and formation mechanism
102 for TEP to the ocean surface (Robinson et al., 2019b)..

103 TEP are highly sticky and provide surfaces for other molecules and bacterial
104 colonization (Passow, 2002b), with between 0.5 and 25% (on average 3%) of marine bacteria
105 being attached to TEP (Busch et al., 2017). TEP naturally aggregate to other particles or highly
106 dense matter and can sink in the ocean to contribute to downward carbon fluxes (Logan et
107 al., 1995;Mari et al., 2017). However, TEP which are not attached to sufficiently dense material
108 will have a resulting low density and rise to the surface to form or stabilize the SML which links
109 the oceans with the atmosphere (Wurl and Holmes, 2008;Wurl et al., 2011).

110 From the ocean surface, TEP have the potential to be transferred to the air. Due to
111 wind and breaking waves, sea spray aerosol particles are formed (de Leeuw et al.,
112 2011;Lewandowska and Falkowska, 2013;Liss and Johnson, 2014) that could be a transfer
113 mechanism for TEP from the ocean to the atmosphere. Recently, high TEP mass
114 concentrations of $1.4 \mu\text{g m}^{-3}$ were reported in ambient marine aerosol particles measured in
115 a size range between 0.1 and $1 \mu\text{m}$, suggesting that gel-like particles can constitute more than
116 half of the particulate OM mass (Aller et al., 2017).

117 Ocean-derived OM, of which TEP is a part, has been reported to be enriched and
118 selectively transferred (compared to sea salt) to the atmosphere (Facchini et al., 2008;Keene
119 et al., 2007;van Pinxteren et al., 2017). Compared to seawater concentrations, organic mass
120 in submicron aerosol particles is strongly enriched by factors of 10^3 and 10^4 (partly up to 10^5)
121 (Quinn et al., 2015 and references therein) due to (not yet in detail resolved) processes during
122 the rise and burst of bubbles at the ocean surface (Blanchard, 1975). The enrichment of OM
123 in supermicron aerosol particles is significantly lower, with average aerosol enrichment factors
124 of 10^2 (Hoffman and Duce, 1976;Keene et al., 2007;Quinn et al., 2015). Aerosol enrichments
125 have been studied for several organic compound groups such as lipids, carbohydrates, and
126 proteins (e.g. Gao et al., 2012;Rastelli et al., 2017;Schmitt-Kopplin et al., 2012;Triesch et al.,
127 2021a;Triesch et al., 2021b;Zeppenfeld et al., 2021). However, at current, data for TEP
128 enrichment in the atmosphere are scarce. Aller et al. (2017) presented TEP mass
129 concentrations in size-resolved aerosol particles and found them to contain more TEP for
130 submicron sizes than for larger sizes. Kuznetsova et al. (2005) reported TEP enrichment of a
131 factor of 40 in freshly produced sea spray. Besides TEP, other types of gel-like airborne
132 particles in the size range of 100 – 300 nm (and even smaller) have been observed, e.g. in the
133 Arctic atmosphere likely originating from the ocean surface (Bigg and Leck, 2008;Leck and
134 Bigg, 2005a, b).

135 In addition to an oceanic transfer, atmospheric in-situ formation might contribute to
136 OM abundance in the atmosphere. Ervens and Amato (2020) provided a framework to
137 estimate the production of secondary biological aerosol mass in clouds by microbial cell
138 growth and multiplication. It was recently shown that this pathway might represent a
139 significant source of biological aerosol material (Ervens and Amato, 2020;Khaled et al.,
140 2021;Zhang et al., 2021). In another recent study, cloud water in-situ formation of amino acids
141 resulting from biotic and abiotic processes has been measured and modelled (Jaber et al.,
142 2021). Moreover, a higher microbial enzymatic activity on the aerosol particles compared to
143 seawater was observed and it was hypothesised that after ejection from the ocean, active
144 enzymes can dynamically influence the OM concentration and composition of marine aerosol
145 particles (Malfatti et al., 2019). Still, the atmospheric in-situ formation of important OM
146 compounds and its importance is not well investigated to date and no studies exist about
147 atmospheric in-situ TEP formation.

148 Regarding the properties of ocean-derived OM in the atmosphere, its ability to act as
149 cloud condensation nuclei (CCN) (Orellana et al., 2011;Sellegrì et al., 2021) or ice nucleating

150 particle (INP) (Burrows et al., 2013;Gong et al., 2020a;McCluskey et al., 2018a;McCluskey et
151 al., 2018b) is not well understood at present. Bigg and Leck, (2008) and Leck and Bigg (2005b)
152 demonstrated, based on morphology and chemical properties, that the biogenic particles
153 collected in air and in the surface microlayer could be consistent with polymer gels. For regions
154 that generally show a low total particle number concentration and low CCN (such as the high
155 Arctic), it was suggested that microgels are CCN (Leck and Bigg, 2005a, b;Orellana et al., 2011),
156 due to their hydrated and hygroscopic nature and due to the absence of other significant
157 aerosol particle sources.

158 In addition, oceanic biogenic INP sources have been discussed (Creamean et al.,
159 2019;Hartmann et al., 2020;Wilson et al., 2015;Zeppenfeld et al., 2019). In regions, however,
160 where other sources dominate, oceanic sources might not suffice to explain the INP
161 population, and non-marine sources most likely significantly contributed to the local INP
162 concentration (Gong et al., 2020a). According to their structure, biopolymers consisting of
163 proteins, lipids, and higher saccharides have been shown to play a role in the ice-nucleating
164 activity (Pummer et al., 2015). In this context, TEP might provide excellent functionalities to
165 act as INP, as they form a 3D network where water molecules can attach, providing a
166 structured surface for ice formation. A direct link between TEP and INP, however, has not yet
167 been experimentally shown in field studies.

168 Within the present study, the number concentrations and size distributions of TEP in
169 the ambient atmosphere in the tropical Atlantic Ocean were elucidated. We aimed at
170 investigating the TEP number concentrations in the ambient aerosol particles and cloud water
171 and to derive connections to oceanic transfer and potential in-situ formation mechanisms.
172 Finally, we compared the TEP number concentrations with recently published atmospheric
173 INP number concentrations at the same location (Gong et al., 2020a) and analyse possible
174 interconnections. To our knowledge, this is the first study with detailed measurements of TEP
175 number size distribution in different atmospheric marine compartments in the tropical
176 Atlantic environment.

177

178 2 Material and methods

179 2.1 Measurement site and ambient sampling

180 Samples were taken during the MarParCloud: “Marine biological production, organic
181 aerosol particles and marine clouds: a Process chain” campaign that took place from
182 September 13th to October 13th 2017 at the Cape Verde archipelago Island Sao Vicente located
183 in the Eastern Tropical North Atlantic (ETNA). A detailed overview of the campaign,
184 background, goals, and first results is available in van Pinxteren et al. (2020). Measurements
185 were performed at the Cape Verde Atmospheric Observatory (CVAO) as described in more
186 detail elsewhere (Triesch et al., 2021a;Triesch et al., 2021b;van Pinxteren et al., 2020). The
187 CVAO is located directly at the shoreline at the northeastern tip of the São Vicente island at

188 10 m a.s.l (Carpenter et al., 2010;Fomba et al., 2014). Due to the trade winds, this site is free
189 from local island pollution and provides reference conditions for studies of ocean-atmosphere
190 interactions as there is a constant north-westerly wind from the open ocean towards the
191 observatory. However, it also lies within the Saharan dust outflow corridor, and mainly in the
192 winter months (January and February), dust outbreaks frequently occur.

193 Total suspended aerosol particle (TSP) for TEP analysis and PM₁₀ sampling for analysis
194 of further aerosol constituents (inorganic ions, INP, dust) was performed on top of a 30 m
195 sampling tower of the CVAO. Tower measurements there mainly represent the conditions
196 above the ocean because the internal boundary layer (IBL), which can form when air passes a
197 surface with changing roughness (i.e. the transfer from open water to island), is mainly
198 beneath 30 m (Niedermeier et al., 2014). During the MarParCloud campaign, the marine
199 boundary layer (MBL) was well mixed as indicated by an almost uniform particle number size
200 distribution within the MBL (Gong et al., 2020b;van Pinxteren et al., 2020). Information on the
201 meteorological conditions during the sampling period is given in **Tab. S1**.

202 TSP were sampled with a filter sampler consisting of a filter holder equipped with a
203 0.2 µm pore-sized, ~~acid-cleaned~~ polycarbonate (PC) filter mounted to a pump. **The PC filters**
204 **had been cleaned with 10% HCl and rinsed with ultrapure water (resistivity=18.2MΩ cm)**
205 **before application**. Sampling usually took place for 24 h and the flow of the pump was
206 between 5 and 10 L min⁻¹ and frequently measured with a flowmeter. Total volumes between
207 10 and 15 m³ were sampled. In seawater TEP analysis, filtration is usually performed at a
208 gentle pressure of 0.2 bar (Engel, 2009) which corresponds to a max flow rate of 21 or 38
209 L min⁻¹. The flow rate of aerosol sampling was max. 10 L min⁻¹ and therefore TEP losses during
210 aerosol particle sampling were not expected.

211 PM₁₀ particles were sampled with a high volume sampler (Digitel, Rieme, Germany)
212 equipped with preheated (105 °C for 24 h) 150 mm quartz fiber filters (Munktell, MK 360) at
213 a flow rate of 700 L min⁻¹, described in detail elsewhere (van Pinxteren et al., 2020). The
214 sampling times for TSP as well as PM₁₀ were usually set to 24 h.

215 Cloud water was sampled on Mt. Verde, which is the highest point of the São Vicente
216 Island (744 m), situated in the northeast of the Island (16°52.11'N, 24°56.02'W) and northwest
217 to the CVAO (van Pinxteren et al., 2020). Again, Mt. Verde experiences direct trade winds from
218 the ocean with no significant influence of anthropogenic activities from the island (Carpenter
219 et al., 2010). Bulk cloud water was collected using a compact Caltech Active Strand Cloudwater
220 Collectors (CASCC2) equipped with acid cleaned Teflon®strands (508 µm diameter). Cloud
221 droplets were caught on the strands and gravitationally channelled into an ~~acid-precleared~~
222 Nalgene bottle. The 50% lower size cut for the CASCC2 is approximately 3.5 µm diameter.
223 Much of the liquid water content (LWC) in clouds is contained of drops between 10 and 30 µm
224 diameter and the CASCC2 is predicted to collect drops in this size range with an efficiency
225 greater than 80% (Demoz et al., 1996).

226 Three cloud water samples collected on the 20.09.2017, the 28.09.2017, and the
227 4.10.2017 were analysed for the TEP number concentrations. They were filtered (150-200 mL)

228 through 0.2 μm pore-sized, ~~acid-cleaned~~ filters for TEP analysis using the same filter type and
229 conditions as applied for the aerosol particle staining. All equipment that was in contact with
230 the cloud water samples (Teflon® strands, sampling bottles, filters) had been cleaned with 10%
231 HCl and rinsed with ultrapure water (resistivity=18.2M Ω cm) before each application as
232 recommended in Engel (2009).
233

234 2.2. Particle sampling from the plunging waterfall tank

235 To investigate a direct oceanic transfer of TEP via bubble bursting, TSP particles were
236 sampled from a plunging waterfall tank experiment that is described in detail in the
237 MarParCloud overview paper (van Pinxteren et al., 2020, SI section). The tank was designed
238 to study the bubble-driven transfer of organic matter from the bulk water into the aerosol
239 phase. It consists of a 1400 L basin with a 500 L aerosol chamber on top. The bubble driven
240 transport of organic matter was induced using a skimmer on a plunging waterfall. A stainless
241 steel inlet was inserted in the headspace of the tank and connected with three filter holders
242 for offline aerosol particle sampling without size segregation (TSP). The filter system for TEP
243 analysis was equipped with a 0.2 μm pore-sized, acid-cleaned polycarbonate (PC) filter
244 mounted to a pump. Sampling usually took place for ~ 24 h, the flow of the pump was between
245 5 and 10 L min^{-1} and frequently measured with a flowmeter. Total volumes between 9 and
246 10 m^3 were sampled. The sampling procedure was therefore identical to the ambient TEP filter
247 sampling. Another filter holder was equipped with a preheated 47 mm quartz fiber filter
248 (Munktell, MK 360) for sodium analysis. The stainless steel inlet was additionally connected
249 to a TROPOS-type Scanning Mobility Particle Sizer (Wiedensohler et al., 2012) for online
250 aerosol measurements. This method of aerosol generation resulted in an efficient generation
251 of nascent sea-spray aerosol particles with an aerosol particle size distribution centred around
252 100 nm (van Pinxteren et al. 2020).
253

254 2.3 Analysis

255 The filters obtained from ambient and tank-generated TSP aerosol particle sampling
256 and cloud water filtrations were stained with 3 mL of an Alcian blue stock solution stained
257 (0.02 g Alcian blue in 100 mL of acetic acid solution, pH 2.5) for 5 s yielding an insoluble non-
258 ionic pigment and afterward rinsed with milliQ water. The dye Alcian blue consists of a
259 macromolecule with a central copper phthalocyanine ring linked to four isothiuronium
260 groups via thioether bonds (Passow and Alldredge, 1995). The isothiuronium groups are
261 strong bases and account for the cationic nature. The exact staining mechanism is not resolved
262 but it is believed that the cationic isothiuronium groups bond via electrostatic linkages (ionic
263 bonds) with the polyanionic molecules of the TEP molecule, hence the carboxylic and sulfonic
264 side groups are stained. Alcian Blue can also react with carbohydrate-conjugated proteins at

265 proteoglycans, but not with nucleic acids and neutral biopolymers (Villacorte et al., 2015).
266 After staining the filters were kept at -20°C and transported to the laboratories of TROPOS.

267 For microscopic analysis, the protocol following Engel (2009) was applied. In short,
268 abundance, area, and size-frequency distribution of TEP were determined using a light
269 microscope (Zeiss Axio Scope A.1) connected to a camera (ColorView III). Filters were screened
270 at 200× magnification. About 10 pictures were taken randomly from each filter in two
271 perpendicular cross-sections (5 pictures each cross-section; dimension 2576 x 1932 pixel, 8-
272 bit color depth) and microscopic pictures of TEP in cloud water are shown in **Fig. 1**. Images
273 were then semi-automatically analyzed using ImageJ (Version 1.44). A minimum threshold
274 value of 16 μm^2 was set for particle size during particle analysis to remove the detection of
275 non-aggregate material by the program. This resulted in a minimum particle size of 4.5 μm
276 (assuming spherical particle).

277 ***Insert Figure 1***

278
279
280 Blank filters were taken for aerosol sampling (inserting filters in the aerosol sampler
281 without probing them) and cloud water (filtering reagent water over a pre-cleaned filter),
282 stained and treated the same way as the microscopic analysis. Blank number concentrations
283 were on average 6% of the cloud water results and between 5% and 20% for aerosol results
284 and the blank values were subtracted from the samples.

285 The analysis of inorganic ions from PM_{10} samples was performed with ion
286 chromatography and conductivity detection. Aqueous extracts of the aerosol samples were
287 made by ca. 25% of the PM_{10} filter in 1.5 mL ultra-pure water (resistivity = 18.2 $\text{M}\Omega\text{ cm}$) for
288 one hour. After the filtration (0.45 μm syringe filter) of the extracts sodium (Na^+), calcium
289 (Ca^{2+}), magnesium (Mg^{2+}), were analyzed by using ion chromatography (Dionex ICS-6000,
290 Thermo Scientific). The cations were separated in an isocratic mode (eluent: 36 mM
291 methanesulfonic acid) on a Dionex IonPac CS16-4 μm column (2×250 mm) that was combined
292 with a Dionex IonPac CG16-4 μm guard column (2×50 mm). The detection limits for the
293 determined ions were between 5 and 20 $\mu\text{g L}^{-1}$ (Zeppenfeld et al., 2021).

294 Non-sea-salt calcium was calculated from the ion ratio of $\text{Ca}^{2+}/\text{Na}^+$ in seawater of
295 0.038 (Turekian, 1968). Dust concentrations were estimated from the aerosol particle mass
296 concentrations as the residual mass after the subtraction of all analytical concentrations from
297 the PM_{10} mass as described elsewhere (Fomba et al., 2014). Trace metal content was
298 determined using a Total Reflection X-Ray Fluorescence (TXRF) S2 PICOFOX (Bruker AXS,
299 Berlin, Germany) spectrometer equipped with a Molybdenum X-ray source (Fomba et al.,
300 2013). The cloud LWC was measured with a particle volume monitor (PVM-100, Gerber
301 Scientific, USA), which was mounted at the same height as the cloud water samplers.

302 INP number concentration (N_{INP}) were measured with two droplet freezing techniques
303 (LINA: Leipzig Ice Nucleation Array and INDA: Ice Nucleation Droplet Array) in different marine

304 compartments. The uncertainties of N_{INP} are given by the 5% to 95% confidence interval and
305 the results are presented in (Gong et al., 2020a).

306 All the samples of this study are summarized in Table 1. In addition to samples from
307 the MarParCloud campaign, surface seawater samples obtained from the ETNA (Engel et al.
308 2020) were considered.

309 ***Insert Table 1***

310 2.4 Enrichment factor

311 To determine enrichment or depletion of TEP in the atmosphere (i.e. on the aerosol
312 particles and in the cloud water) in relation to the TEP concentration in the ocean water, the
313 concept of the aerosol enrichment factor can be applied. To this end, the concentration of the
314 compound of interest in each compartment is related to the respective sodium mass
315 concentration, as sodium is regarded as a conservative sea salt tracer transferred to the
316 atmosphere in the process of bubble bursting (Sander et al., 2003). This concept is usually
317 applied for calculating the enrichment of a compound in the aerosol particles ($EF_{aer.}$) in relation
318 to seawater (Quinn et al., 2015), but was recently extended to calculate the enrichment of
319 organic compounds in cloud water (EF_{cloud}) in relation to seawater (Triesch et al., 2021a).
320 Therefore, in the following the enrichment factor is defined as $EF_{atm.}$ (atmosphere
321 enrichments factor) in equation 1.

322

$$323 EF_{atm.} = \frac{c(TEP)_{atm}/c(Na^{+}mass)_{atm}}{c(TEP)_{seawater}/c(Na^{+}mass)_{seawater}} \quad (1)$$

324

325 For equation (1), TEP number concentrations were converted to TEP volume
326 concentrations. To this end, for atmospheric and for oceanic samples, particle number
327 concentrations of TEP were extracted from the size distribution spectra and volume
328 concentrations were calculated (assuming spherical particles). More detail on the conversion
329 can be found in the SI (Tab. S2-S5).

330

331 3 Results and Discussion

332 3.1 Concentration and size distribution of TEP

333 Within the three-weeks sampling period, TEP varied within one order of magnitude
334 between 7×10^2 and 3×10^4 #TEP m^{-3} in the aerosol particles and between 4×10^6 and 9×10^6
335 #TEP L^{-1} in the cloud water (analysed diameter size range: ~ 4.5 to ~ 30 μm) as shown in **Fig. 2**.
336 The cloud water concentrations were converted to atmospheric concentrations using the
337 measured LWC of the cloud water (0.39 $g\ m^{-3}$) and resulted in concentrations of $2 - 4 \times 10^3$
338 #TEP m^{-3} (**Tab. S4**). ~~As a result, a striking similarity (agreement within one order of magnitude)~~
339 ~~for TEP concentrations in the aerosol particles (average: 1×10^4 #TEP m^{-3} , Tab. S2) and the cloud~~
340 ~~water (average: 0.3×10^4 #TEP m^{-3} , Tab. S4) was found, suggesting that the majority of the TEP~~

341 ~~particles are activated to cloud droplets when a cloud forms.~~ Comparing the #TEP
342 concentrations in cloud water to the ones in the ambient aerosol particles suggested that
343 about 20% of the ambient TEP particles are activated to cloud droplets when a cloud forms.

344 *Insert Figure 2*

345

346 In addition, TEP were measured in four aerosol particle samples from the plunging
347 waterfall tank and the concentrations varied between 4×10^2 and 3×10^3 #TEP m^{-3} (Tab. S3).
348 While the TEP concentrations in ambient aerosol particle and cloud water were not
349 significantly different (ANOVA, oneway, $p = 0.054$ at a 0.05 level), the tank-generated TEP
350 concentrations were significantly lower than the ambient aerosol TEP concentrations (ANOVA,
351 oneway, $p = 0.004$ at a 0.05 level). The TEP number concentrations measured in the different
352 atmospheric compartments, the ambient aerosol particles, the tank-generated aerosol
353 particles and the cloud water are summarized in Fig. 3a and the individual values are
354 presented in the Tab. S2-S4.

355 *Insert Figure 3*

356

357 ~~Besides for~~ In addition to the total number concentrations, TEP number size
358 distribution were derived from all ambient aerosol particle samples and are shown in Fig. 4
359 (a-d) in both, linear and logarithmic form. In addition, the TEP number size distribution of one
360 cloud water sample is presented in Fig. 4 (e, f). All samples exhibited very similar trends in
361 their size distribution, with higher number concentrations for smaller sizes.

362 *Insert Figure 4*

363

364 From the observed size distributions, it can be assumed that the number
365 concentrations will continue to increase toward smaller sizes. A comparison of TEP number
366 concentrations in the ambient aerosol particles or cloud water to literature values is
367 challenging due to the availability of very few studies and different sample types and size
368 ranges regarded in different studies. However, the here observed trend in the TEP number
369 size distributions is consistent with studies from Kuznetsova et al. (2005) showing increased
370 TEP concentrations in simulated sea spray regarding particle sizes from $50 \mu\text{m}$ to $10 \mu\text{m}$ in
371 diameter. In addition, TEP mass concentrations showed a similar trend with higher
372 concentrations towards smaller particle sizes (size range $0.1\text{-}1 \mu\text{m}$, Aller et al. (2017)), that
373 was, however not as pronounced as for TEP number concentrations observed here.

374 Regarding polymer gels in general, a strong increase with decreasing sizes was
375 ~~observed for the polymer gels~~ in cloud water in the high Arctic (north of 80°N) in late summer
376 using a very sensitive microscopic technique with epifluorescence (Orellana et al., 2011).
377 2×10^9 micrometer-sized polymer gels per mL^{-1} and $2 - 6 \times 10^{11}$ nanometer-sized polymer gels

378 per mL⁻¹ were observed and the majority of the particles were smaller than 100 nm (Orellana
379 et al., 2011). The measurements from Orellana et al. (2011) regarded a much smaller particle
380 diameter range (down to nm scale) compared to the present work and are therefore not
381 directly comparable. However, from the logarithmic TEP number concentration vs. diameter
382 relationship (**Fig. 4**) we calculated TEP number concentrations for smaller particle ranges (sub-
383 micrometer size range). TEP number concentrations between 4.2×10^4 #TEP m⁻³ (low “TEP5”
384 case, equation from **Fig. 4b**) and 1.6×10^6 #TEP m⁻³ (high “TEP10” case, equation from **Fig. 4d**)
385 are calculated for PM₁ particles. The high but varying concentrations for the two cases
386 underlines the need for more measurements in the submicron range to derive robust
387 numbers. Similarly, a concentration of 3.0×10^8 #TEP L⁻¹ for PM₁ particles in cloud water were
388 calculated and 2.1×10^{10} #TEP L⁻¹ for PM_{0.2} particles might exist in the submicron-size range
389 (following the equation from **Fig. 4f**).

390 These calculations show that the number of gel-like particles in the high Arctic was still
391 several orders of magnitudes higher compared to TEP particles in the tropical Atlantic, e.g.
392 10^{10} #TEP L⁻¹ (200 nm particles) in tropical cloud water observed here vs. 10^{11} #polymer gels
393 per mL⁻¹ (= 10^{14} #polymer gels per L⁻¹) from Orellana et al. (2011). If the TEP particles in the
394 tropical atmosphere comprise only a small subgroup of the total polymer gel number, or if the
395 total amount of gel-like particles is generally higher in Polar Regions remains to be
396 investigated.

397 3.2 Relating atmospheric TEP to the ocean

398 From a recent study of TEP number concentrations in different oceanic regions, TEP number
399 concentrations in surface waters (10 m depth) of the East Tropical North Atlantic (ETNA) were
400 obtained (Engel et al., 2020). ETNA is the region that geographically includes the Cape Verde
401 islands. The oceanic TEP number concentrations are shown in **Fig. 5** and are discussed in more
402 detail in Engel et al. (2020). The TEP in the ocean showed a similar size distribution compared
403 to the TEP in the atmosphere (i.e. aerosol particles and cloud water, **Fig. 4**) with increasing
404 TEP number concentrations toward smaller particle sizes (**Tab. S5** and more details in Engel et
405 al. (2020)).

406

407 *Insert Fig. 5*

408

409 A detailed comparison of #TEP in the ocean and in the atmosphere regarding the
410 identical size bins showed that the #TEP distribution among the different size bins were much
411 more balanced for seawater than for aerosol particles. In aerosol particles, on average 51% of
412 the #TEP were located in the smallest analysed size bin (4.5-7 μm) and show a sharp decrease
413 towards the second size bin (that contained 24% of the TEP) (Fig. 6). For the seawater TEP,
414 however, around 35% of the #TEP were found in the first size bin and the relative contribution
415 decreased uniformly towards the larger size bins (Fig. 6). This distribution is also visible in the
416 correlation curves of Fig 4 (b,d,f) and Figure 5b. The correlation curves for the aerosol particles

417 (and cloud water) have a steeper slope compared to the curve obtained for seawater TEP. This
418 could imply that i) the transfer of TEP from the ocean to the atmosphere is most efficient for
419 small size ranges, ii) larger TEP are converted to smaller TEP in the atmosphere (e.g. break
420 down), and /or iii) atmospheric in-situ formation mechanism of TEP preferably occur in smaller
421 particle size ranges. These considerations will be further evaluated in section 3.3.

422

423 ***Insert Figure 6***

424

425 ~~Ocean water, atmospheric particles, and cloud water are different marine~~
426 ~~compartments and to~~ To compare seawater and atmospheric TEP concentrations in terms of
427 enrichment or depletion, the atmospheric enrichment factor $EF_{atm.}$ (Equation 1) was
428 calculated. However, the TEP number concentrations in the ocean surface water were
429 obtained from an additional measurement campaign, taking place in the biologically
430 productive Mauritanian Upwelling region in the year 2012, hence at another time and season
431 (Tab. 1). Compared to other oceanic regions, the TEP values from the Mauritanian Upwelling
432 region were at the higher end (Engel et al., 2020). The region around the CVAO is rather
433 oligotrophic and Chlorophyll-a values during the MarParCloud campaign were relatively low
434 with 0.1 up to 0.6 $\mu\text{g L}^{-1}$ (van Pinxteren et al., 2020). As TEP production is often connected to
435 phytoplankton activity, the TEP concentration at the CVAO might be lower compared to more
436 productive regions (Robinson et al., 2019a). A previous study showed the total TEP number
437 concentrations (covering TEP sizes between 1 and 200 μm) at the Cape Verde islands (south
438 of São Vicente at 16°44.4'N, 25°09.4'W) were by a factor of 2 lower than the data reported
439 here, in detail $0.9 \times 10^7 \text{ L}^{-1}$ (Engel et al., 2015) vs. $2 \times 10^7 \text{ L}^{-1}$ (Tab. S5). Lower TEP concentrations
440 would result in higher $EF_{atm.}$ (Equation 1) regarding the ambient as well as the tank
441 measurements as the same type of seawater was used for the calculations. Hence, the here
442 reported $EF_{atm.}$ represent lower limits.

443 In order to compare the same TEP diameters in all compartments, the size range
444 between 5 μm (lower limit for atmospheric measurements) and 10 μm (typical upper limit for
445 ambient aerosol particles) was regarded and converted from number to volume concentration
446 (more details in Table S2-S4 and Fig. S1). For ocean water, TEP number concentrations of
447 $3.5 \times 10^3 \text{ \#TEP mL}^{-1}$ ($= 3.5 \times 10^6 \text{ \#TEP L}^{-1}$) and a TEP volume concentration of $4.6 \times 10^5 \mu\text{m}^3 \text{ TEP mL}^{-1}$
448 ($= 3.5 \times 10^8 \mu\text{m}^3 \text{ TEP L}^{-1}$) were obtained. The respective values for the TEP volume
449 concentration of ambient and tank-generated aerosol particles, as well as for the cloud water
450 are listed in Tables S2-S4 and illustrated in Fig 3b. As mentioned above, the factors given here
451 are subject to some uncertainties and represent lower limits. An error discussion is introduced
452 in the Supporting Information as an appendix to Table S2. It is clearly visible that the $EF_{aer.}$
453 *ambient* are significantly higher than the $EF_{aer. tank}$ (ANOVA, oneway, $p = 0.0017$ at a 0.05 level)
454 with average values of 9×10^3 and 50, respectively. The average EF_{cloud} was 1×10^3 . This means
455 that the enrichment of TEP derived from the plunging waterfall tank, representing the bubble-

456 bursting transfer, is about two orders of magnitude lower compared to the enrichment of TEP
457 in the ambient aerosol particles.

458 It should be noted that the lower enrichment in the tank resulted from the lower TEP
459 number concentrations in the generated aerosol particles, as the particulate sodium
460 concentrations in the tank aerosol were even higher than in the ambient particles (Tab. S3).
461 This suggests that, although an artificial tank study cannot represent the ambient
462 environment, the generation of sea spray aerosol was in progress; however, TEP transfer
463 seemed to be not pronounced.

464 In the following, the here obtained enrichment factors will be discussed in more detail
465 considering studies available from literature.

466 Atmospheric enrichment of ocean-derived OM, have often been reported (e.g.
467 Facchini et al., 2008;Keene et al., 2007;O'Dowd et al., 2004;Schmitt-Kopplin et al.,
468 2012;Triesch et al., 2021a;Triesch et al., 2021b;van Pinxteren et al., 2017). Submicron particles
469 are usually strongly enriched with ~~organic matter~~ OM with aerosol enrichment factors $EF_{aer.}$
470 of 10^3 up to 10^5 (Quinn et al., 2015 and references therein). The enrichment in supermicron
471 aerosol particles is, however, significantly lower. Laboratory studies showed enrichment of
472 OM in the order of 10^2 (Hoffman and Duce, 1976;Keene et al., 2007;Quinn et al., 2015). From
473 the MarParCloud campaign, enrichment factors of free amino acids were between 10 and 30
474 in ambient supermicron particles (Triesch et al. 2021a). Kuznetsova et al. (2005) reported TEP
475 enrichments in freshly produced sea spray with $EF_{aer.} = 44 \pm 22$ based on TEP number
476 concentration. Consequently the here reported $EF_{aer. tank}$ (50 ± 35) are well in-line with
477 published enrichment factors for OM in general and TEP specifically. However, the $EF_{aer. ambient}$
478 (9×10^3) were orders of magnitude higher than reported enrichment factors for supermicron
479 aerosol particles. Enrichment factors of OM in cloud water are hardly available; we recently
480 reported an enrichment of $10^3 - 10^4$ of free amino acids in cloud water from the MarParCloud
481 campaign (Triesch et al., 2021a) that were higher than the here observed EF_{cloud} .

482 The concept of the aerosol enrichment factor originally originates from controlled tank
483 experiments where a direct transfer of compounds from the ocean via sea-spray aerosol
484 formation occurs. Obviously, this does not automatically correspond to the ambient
485 environment as mixing processes, aging, and further transformation reactions are not
486 accounted for. However, the $EF_{aer. ambient}$ which is much bigger than ~~$EF_{aer.}$~~ $EF_{aer. tank}$ and the
487 comparison of EF_{cloud} towards former literature data clearly show the presence of significantly
488 more TEP in ambient aerosol and cloud water compared to oceanic seawater which will be
489 discussed in detail in the following section.

490

491 3.3 Possible sources and atmospheric formation pathways of TEP

492

493 3.3.1 Primary TEP sources

494

495 The high abundance of TEP in the aerosol particles and cloud water might correspond
496 to an oceanic transfer within the process of bubble bursting. To investigate a linkage to the
497 bubble bursting transfer, TEP concentrations were correlated to the wind speed, as well as to
498 the sea-spray tracers sodium and magnesium. To account for biases due to a number-based
499 (TEP) and mass-based (sodium, magnesium) comparison, the particle volume of TEP was
500 calculated from the particle number concentrations (regarding the size range: 5-10 μm). To
501 this end, from each particle diameter within a size range of 5-10 μm , the respective volume
502 was determined, assuming spherical particles, and summed up (data in **Tab. S2**). This
503 transformation accounts for the fact that big TEP particles likely possess a large mass but a
504 low number concentration and vice versa.

505 Reasonably good correlations of TEP to sodium, sea-salt calcium (Ca_{ss}) and magnesium,
506 ($R^2 = 0.5$, **Fig. 7a-c**) were found, suggested some connection to a bubble bursting transfer.
507 However, a correlation of TEP to wind speed was not found. It may be that since wind speed
508 data represented an average value of 24 hours, short but pronounced changes in the wind
509 speed were not visible in the average wind speed value. No correlation was found between
510 TEP and non-sea-salt calcium as well as total calcium (**Fig. 7d**).

511

512 ***Insert Figure 7***

513

514 Despite this correlation of TEP to sea spray tracers, the high abundance and
515 enrichment of #TEP in the ambient aerosol particles compared to literature data (Kuznetsova
516 et al., 2005) and compared to the concentration and enrichment of the #TEP from the plunging
517 waterfall tank performed here, suggests that additional (secondary) TEP sources in the
518 ambient atmosphere exist from which TEPs are added to their primary transfer by bubble
519 bursting from the oceans. At the Cape Verde islands, besides the ocean, mineral dust is an
520 important aerosol particle source (Fomba et al., 2014). TEP are generally attributed to be
521 ocean-derived compounds however, dust has often been reported to transport attached
522 biological particles (Maki et al., 2019; Marone et al., 2020). During the MarParCloud campaign,
523 dust influences were low to moderate and the aerosol particle mass was found to be
524 predominantly of marine origin (Fomba et al., 2014; van Pinxteren et al., 2020). Some dust
525 influences were visible though, e.g. variations in the particle number concentrations, with
526 elevated concentrations on (even low) dust influenced air masses (Gong et al., 2020b). TEP
527 number concentrations showed no clear connection to the ambient dust concentrations (**Fig.**
528 **2**). Within periods of moderate dust, TEP were partly below the detection limits (on
529 26.09.2017) and partly exhibited high concentrations (e.g. on 28. and 29.09.2017). A
530 correlation between TEP and dust was not found ($R^2 = 0.05$, **Fig. 7e**) therefore, we do not
531 consider dust to be a transport medium for TEP to the particles or cloud water. However, dust
532 might play a role in abiotic TEP formation, as discussed in chapter 3.3.2.1.

533

534 3.3.2. In-situ formation

535

536 3.3.2.1 Abiotic formation

537

538 In aquatic environments, abiotic TEP formation has been reported to happen via several
539 pathways, including spontaneous assembly from TEP precursors (Passow, 2002b). The aerosol
540 particle and cloud water samples from the MarParCloud campaign investigated here showed
541 high mass concentrations of amino acids (up to 6.3 ng m⁻³ in the submicron aerosol particles
542 and up to 490 ng m⁻³ in the cloud water, published in Triesch et al. (2021a)) as well as
543 dissolved polysaccharides (up to 2 ng m⁻³ in the submicron aerosol particles and up to 2400
544 ng m⁻³ in the cloud water, results in preparation for publication). In the ocean, the dissolved
545 polysaccharides are known TEP precursors (Passow, 2002b) and Wurl et al. (2011) determined
546 abiotic TEP formation rates from dissolved polysaccharide concentration in various oceans.
547 The rates were on average $7.9 \pm 5.0 \mu\text{mol C L}^{-1} \text{d}^{-1}$ and therefore significant considering that
548 the average TEP concentration was $18.1 \pm 15.9 \mu\text{mol C L}^{-1}$ and the average dissolved
549 polysaccharide concentration was $12.2 \pm 3.8 \mu\text{mol C L}^{-1}$ in the surface seawater (Wurl et al.,
550 2011). Robinson et al. (2019b) showed that rising bubbles can lead to an enhanced TEP
551 formation already after some minutes. The lifetime of supermicron aerosol particles, to which
552 the TEP particles studied here belong, are between hours and days, for example, Madry et al.
553 (2011) calculated an average lifetime of supermicron sea salt particles of 50 hours. Hence
554 abiotic TEP formation processes lie within the lifetime of supermicron aerosol particles and
555 we suggest that spontaneous TEP formation from the (high) abundant dissolved
556 polysaccharides likely contributed to the high TEP concentrations observed in the ambient
557 atmosphere in the present study. However, it needs to be considered that the abiotic TEP
558 formation processes described by Wurl et al. 2011 and Robinson et al. were relevant for the
559 oceanic environment and might not directly translated to atmospheric processes. Further
560 studies are required on this topic.

561 Another important parameter likely impacting TEP formation is the presence of
562 mineral dust. As already discussed above, dust mass concentrations were low to moderate,
563 however not negligible, during the MarParCloud campaign. In laboratory minicosm studies,
564 the addition of dust to oceanic water resulted in an acceleration of the kinetics of TEP
565 formation leading to the formation of fast sinking particles (Louis et al., 2017). This process
566 likely happens due to particle aggregation, meaning that dissolved OM and dust aggregate to
567 form TEP (Louis et al., 2017). In addition, dust particles in cloud water might promote
568 turbulence, which, in aquatic media, has been suggested to enhance abiotic TEP formation
569 (Passow, 2002b). The dust deposition at the Cape Verdes has been recognized as a potentially
570 large contributing factor to the TEP enrichment in the SML at the Cape Verdes (Robinson et
571 al., 2019a). Here, we speculate that even low concentrations of mineral dust can influence the
572 TEP formation on the aerosol particles and in the cloud water. This is further supported by the
573 microscopic detection of dust in the cloud water (Fig. 1), that likely enhance the possibility
574 that particles in the cloud water collide and stick. Consequently, while dust did not seem to

575 serve as a transport medium for TEP (see sec. 3.3.1), dust may contribute to in-situ TEP
576 formation in cloud water due to abiotic particle aggregation.

577 From atmospheric studies, marine gel particles have been reported to undergo a
578 volume phase transition in response to environmental stimuli, such as pH and temperature as
579 well as cleavage of their polymers due to UV radiation (Orellana et al., 2011). UV radiation can
580 break down microgels in the ocean to a high number of smaller (nano-sized) particles (Orellana
581 and Verdugo, 2003) – a mechanism that is expected highly relevant in the atmosphere where
582 UV radiation is higher than in seawater. Furthermore, it has been shown that a lowering of
583 the pH from neutral conditions (7 or 8) to 4.5 causes a sudden transition of gel particles in
584 which the polymer network collapsed to a dense, non-porous array (Chin et al., 1998). ~~The pH~~
585 ~~in the cloud water analysed here was between 6.3 and 6.6.~~ As TEP are reported to exhibit a
586 gel-like character (Passow, 2002b), volume and number concentrations might be affected by
587 the **different factors such as** pH, ion density, temperature and pressure in the atmosphere.
588 **The measured cloud water pH-value of the samples analysed here was between 6.3 and 6.6,**
589 **at which marine gels could split into smaller units (Chin et al., 1998). Hence, a part of the cloud**
590 **water TEP might be below the minimum detectable particle size of 4.5 μm due to the slightly**
591 **acidic conditions.** This could explain the lower concentrations in cloud water ($2 - 4 \times 10^3$
592 \#TEP m^{-3}) compared to ambient aerosol particles ($7 \times 10^2 - 3 \times 10^4$ \#TEP m^{-3}). Hence, the
593 different environmental stimuli likely impact atmospheric TEP formation and might lead to
594 the formation of smaller particles. However, from our data we cannot **fully explain the role of**
595 **each of these effects** and such investigations warrant further studies.

596 3.3.2.2 Biotic formation

597
598 Besides abiotic pathways, in aqueous media, TEP can be directly released as
599 particulates from aquatic organisms involving phytoplankton and bacteria (Passow, 2002a)
600 Biotic TEP formation has by now been studied for seawater and lakes (Passow, 2002a)
601 however, bacteria are also present in the atmosphere and likely transferred from the ocean
602 via sea spray (Rastelli et al., 2017) and can survive in cloud droplets (Deguillaume and al.,
603 2020). The bacterial abundance in cloud water samples taken at Mt. Verde during the
604 MarParCloud campaign ranged between 0.4 and 1.5×10^5 cells mL^{-1} (van Pinxteren et al., 2020).
605 This concentration is one to two orders of magnitude higher than the TEP concentrations. The
606 bacterial tracer muramic acid (Mimura and Romano, 1985) was detected in the aerosol
607 particles and cloud water sampled here in considerable concentrations (~ 25 nM, data not
608 shown), strongly suggesting bacterial activity in cloud water. We cannot derive conclusions on
609 the origin of the bacteria measured in cloud water reported here, however the transfer of
610 bacteria from the ocean to the atmosphere has been shown before (Rastelli et al.,
611 2017; Uetake et al., 2020). TEP are known to be closely connected to bacteria in different ways
612 (Passow, 2002b; Passow, 2002a), therefore, the presence of bacteria in the atmosphere
613 exhibits a potential source of cloud water TEP observed here. Furthermore, TEP are strongly
614 colonized by bacteria (Busch et al., 2017; Zäncker et al., 2019). Hence, TEP can be a transfer

615 vector for bacteria from the ocean to the atmosphere and/or act as a medium for bacterial
616 colonisation in marine clouds.

617 The presence of active enzymes on ambient aerosol particles (enriched compared to
618 seawater) and therefore biogenic in-situ cycling of OM through enzymatic reactions in
619 atmospheric particles was recently suggested (Malfatti et al., 2019). This is well in-line with
620 the findings that the aerosol particles and cloud water from the MarParCloud campaign
621 contained high concentrations of OM (amino acids, lipids), assumingly connected to the
622 biogenic formation (Triesch et al., 2021a;Triesch et al., 2021b). A combined approach of
623 laboratory experiments and modelling recently underlined the importance of biotic (and
624 abiotic) formation processes of OM in clouds (Jaber et al., 2021).

625 Regarding time scales of biotic processing, Matulova et al. (2014) showed that the
626 *Bacillus* sp. 3B6 isolated from cloud water was able to bio-transform saccharides that are
627 present in the atmosphere. The saccharides formed exopolymer substances (EPS), of which
628 TEP are a subgroup. The formation of EPS was revealed after 48 h of incubation and therefore
629 within the lifetime of supermicron aerosol particles (Madry et al., 2011).

630 Considering recent literature and the data reported here, we suggest that in-situ TEP
631 formation related to biogenic processes and likely connected to bacteria, as reported for
632 seawater, are important in the marine atmosphere as well. Besides, although not measured
633 here, microalgae and cyanobacteria, that are relevant for direct TEP formation in seawater,
634 have been reported to occur in the atmosphere (e.g. Lewandowska et al., 2017;Sharma et al.,
635 2007;Wiśniewska et al., 2019;Wiśniewska et al., 2022). It is worth studying, if these species
636 and their metabolic degradation products contribute to atmospheric TEP processing.

637

638 3.4 Connecting TEP and Ice nucleating particles (INP)

639 Different kinds of ice-nucleating macromolecules have been found in a certain range
640 of biological species and consist of a variety of chemical structures including proteins,
641 polysaccharides (Pummer et al., 2015) and lipids (DeMott et al., 2018). TEP, consisting of
642 polysaccharidic chains, bridged with divalent cations, may therefore possess good properties
643 to act as INP, however, such a link has not yet been shown in field experiments.

644 During the MarParCloud campaign INP number concentration (N_{INP}) was measured in
645 different marine compartments and the results are presented in Gong et al. (2020a). By
646 combining INP concentration in the seawater, aerosol particles and cloud water, it was found
647 that N_{INP} in the atmosphere were at least four orders of magnitude higher than what would
648 be expected if all airborne INP would originate from sea spray. The measurements indicated
649 that other sources besides the ocean, such as mineral dust or other long-ranged transported
650 particles, contributed to the local INP concentration. However, some indications for
651 contributions of biological particles to the INP population were obtained (details in Gong et
652 al., 2020a). Nevertheless, the sources of INP could not be revealed in detail.

653 In the present study, quantitative INP data (presented in Gong et al. 2020a) and TEP
654 data measured from the same campaign were compared. To this end, INP concentrations
655 achieved from PM₁₀ quartz-fiber filters taken at the CVAO during the same period as the TSP
656 filters were compared with the TEP measurements. In addition, cloud water INP and TEP data
657 obtained from the same samples were combined.

658 TEP number concentrations were on average between $10^3 - 10^4 \text{ m}^{-3}$ in the ambient
659 aerosol particles, whereas INP number concentrations at -15°C were between $10 - 10^2 \text{ m}^{-3}$
660 (Gong et al., 2020a). It is interesting to note that the TEP concentrations in the ambient aerosol
661 particles were about two orders of magnitude higher compared to INP concentrations. Similar
662 findings were obtained for the cloud water comparisons; TEP concentrations ($\sim 10^6 \text{ L}^{-1}$) were
663 on average two orders of magnitude higher than INP number concentrations at -15°C in cloud
664 water ($\sim 10^4 \text{ L}^{-1}$) (Gong et al., 2020a).

665 The correlation between INP (active at -15°C) and TEP concentrations was weak with
666 $R^2 = 0.3$ (Fig. 7f), showing that a direct link between INP and the entire TEP number
667 concentrations was not very pronounced. It needs to be underlined that TEP concentrations
668 below a particle size of $4.5 \mu\text{m}$ are not included here and according to the size distribution,
669 the TEP concentrations are increasing towards smaller sizes. Most of the here reported TEP
670 particles were in the **supermicron size range between $\sim 4.5 - 14 \mu\text{m}$** (Fig. 4). However, the
671 biologically active N_{INP} at the Cape Verdes were mainly present in the supermicron mode (> 1
672 μm) (Gong et al., 2020a), hence a comparison with the TEP particle concentrations above 5
673 μm seems justified. Nevertheless, future studies should concentrate on the exact same size
674 ranges for TEP and INP.

675 The INP functionalities of biomolecules are not straightforward and whether a
676 macromolecule acts as INP is depending on many factors, as its size, proper position of
677 functional groups, and their allocation (Pummer et al., 2015). Typically, not the entire surface
678 of an INP but rather specific areas (active sites) participates in ice nucleation. This means that
679 despite TEP likely providing INP properties, only a fraction of TEP, if any, might be able to act
680 as INP. This hypothesis is supported by the findings that marine gels exhibit hydrophobic and
681 hydrophilic surface-active segments, strongly suggesting a dichotomous, non-uniform
682 behaviour of polymer gels (Leck et al., 2013; Orellana et al., 2011; Ovadnevaite et al., 2011). As
683 mentioned in 3.3.2.1 and 3.3.2.2, TEP are often attached to, or colonized with bacteria.
684 Bacteria itself, have been shown to provide excellent INP functionalities (Pandey et al., 2016)
685 and TEP might act as a carrying medium for INP, such as bacteria. Bacteria concentrations
686 were higher than TEP concentrations and also higher than INP concentrations. However, only
687 a fraction of all bacteria ($0.5 - 25\%$) is associated with TEP and, vice versa, not all TEP are
688 colonized by bacteria (Passow, 2002b). There is an indication that especially in oligotrophic
689 waters, as are the Cape Verde islands, the fraction of bacteria attached to TEP is comparably
690 low (Schuster and Herndl, 1995). Hence, the concentration range of bacteria-colonized TEP in
691 relation to INP is worth further consideration. This might help to unravel if a functional
692 relationship between bacteria-colonized TEP and INP exists and if a certain part of TEP contain

693 fragments in the biological INP population that, beyond dust, play a role in the Cape Verde
694 atmosphere.

695

696 4 Conclusion

697

698 This study presented TEP number concentrations $> 4.5 \mu\text{m}$ in ambient atmospheric samples
699 from the tropical Atlantic Ocean during the MarParCloud campaign as well as in generated
700 atmospheric particles using a plunging waterfall tank. The atmospheric TEP showed a similar
701 size distribution compared to the TEP in the ocean with increasing TEP number concentrations
702 toward smaller particle sizes, however the #TEP distribution among the different size bins
703 were much more balanced for seawater than for aerosol particles where half of the #TEP were
704 located in the smallest analysed size bin (4.5-7 μm). Based on Na^+ concentrations in seawater
705 and the atmosphere, the enrichment of TEP in the tank generated aerosol particles was well
706 in-line with another study. The TEP enrichments in the ambient atmosphere were, however,
707 up to two orders of magnitude higher compared to the tank study and such high values are
708 thus far not reported for supermicron aerosol particles. We speculate that the high
709 enrichment of TEP in supermicron ~~the~~ particles and in cloud water result from a combination
710 of enrichment during bubble-bursting transfer from the ocean and **secondary** in-situ
711 atmospheric formation. We propose that similar (biotic and abiotic) formation mechanism
712 reported for TEP formation in the (sea)water might take place in the atmosphere as well, as
713 the required conditions (e.g. high concentrations of dissolved TEP precursors such as
714 polysaccharides, presence of bacteria in the cloud water) were given. An assessment of the
715 importance of the biotic versus the abiotic TEP formation pathways in the atmosphere,
716 however, needs further investigations. TEP concentrations in the atmosphere were two orders
717 of magnitude higher than INP concentrations in the aerosol particles and cloud water,
718 respectively. However, only a part of the TEP population, assumingly the one colonized by
719 bacteria, might contribute to INP population, and are worth further studies. Finally, while dust
720 might be a dominant INP source in the here investigated tropical Atlantic region close to the
721 Saharan desert, in other remote oceanic locations, marine gel particles, their in-cloud
722 formation and connection to bacteria **and phytoplankton** in the atmosphere could be highly
723 relevant for a better understanding of marine cloud properties.

724

725 Data availability

726 The TEP data are accessible under the following link
727 <https://doi.pangaea.de/10.1594/PANGAEA.938169>. INP concentrations are accessible under
728 the following link: <https://doi.pangaea.de/10.1594/PANGAEA.906946>.

729 Special issue statement

730 Acknowledgement

731 We acknowledge the funding by the Leibniz Association SAW in the project “Marine biological
732 production, organic aerosol particles and marine clouds: a Process Chain (MarParCloud)”
733 (SAW-2016-TROPOS-2), the Research and Innovation Staff Exchange EU project MARSU
734 (69089) and the Deutsche Forschungsgemeinschaft (DFG, German Research Foundation) –
735 Projektnummer 268020496 – TRR 172, within the Transregional Collaborative Research
736 Center “Arctic Amplification: Climate Relevant Atmospheric and Surface Processes, and
737 Feedback Mechanisms (AC)³” in sub-projects B04. We thank the CVAO site manager Luis Neves
738 as well as René Rabe and Susanne Fuchs for technical and laboratory assistance. We further
739 acknowledge the professional support provided by the Ocean Science Centre Mindelo (OSCM)
740 and the Instituto do Mar (IMar).

741

742 Author contributions

743 MvP led the MarParCloud campaign and, together with the campaign participants KWF, XG,
744 EB, NT, BR, FS and HW performed the aerosol particle and cloud water sampling at the Cape
745 Verde island. EB designed and operated the plunging waterfall tank. BR performed the
746 microscopic TEP measurements and XG made the INP analysis. AE contributed the seawater
747 TEP data. MvP performed the data interpretation with help from SZ and BR. MvP wrote the
748 manuscript with contributions from all authors.

749 Competing interest

750 The authors declare that they have no conflict of interest.

751

752 References

753 Alldredge, A. L., Passow, U., and Logan, B. E.: The abundance and significance of a class of
754 large, transparent organic particles in the ocean Deep-Sea Research Part I-Oceanographic Research
755 Papers, 40, 1131-1140, 10.1016/0967-0637(93)90129-q, 1993.

756 Aller, J. Y., Radway, J. C., Kiltbau, W. P., Bothe, D. W., Wilson, T. W., Vaillancourt, R. D., Quinn,
757 P. K., Coffman, D. J., Murray, B. J., and Knopf, D. A.: Size-resolved characterization of the
758 polysaccharidic and proteinaceous components of sea spray aerosol, *Atmos. Environ.*, 154, 331-347,
759 10.1016/j.atmosenv.2017.01.053, 2017.

760 Bigg, E. K., and Leck, C.: The composition of fragments of bubbles bursting at the ocean
761 surface, *Journal of Geophysical Research-Atmospheres*, 113, 10.1029/2007jd009078, 2008.

762 Bittar, T. B., Passow, U., Hamaraty, L., Bidle, K. D., and Harvey, E. L.: An updated method for
763 the calibration of transparent exopolymer particle measurements, *Limnol. Oceanogr. Meth.*, 16, 621-
764 628, 10.1002/lom3.10268, 2018.

765 Blanchard, D. C.: Bubble Scavenging and the Water-to-Air Transfer of Organic Material in the
766 Sea, in: Applied Chemistry at Protein Interfaces, Advances in Chemistry, 145, American Chemical
767 Society, 360-387, 1975.

768 Burrows, S. M., Hoose, C., Poschl, U., and Lawrence, M. G.: Ice nuclei in marine air: biogenic
769 particles or dust?, Atmospheric Chemistry and Physics, 13, 245-267, 10.5194/acp-13-245-2013, 2013.

770 Busch, K., Endres, S., Iversen, M. H., Michels, J., Nothig, E. M., and Engel, A.: Bacterial
771 Colonization and Vertical Distribution of Marine Gel Particles (TEP and CSP) in the Arctic Fram Strait,
772 Frontiers in Marine Science, 4, 10.3389/fmars.2017.00166, 2017.

773 Carpenter, L. J., Fleming, Z. L., Read, K. A., Lee, J. D., Moller, S. J., Hopkins, J. R., Purvis, R. M.,
774 Lewis, A. C., Müller, K., Heinold, B., Herrmann, H., Fomba, K. W., van Pinxteren, D., Müller, C., Tegen,
775 I., Wiedensohler, A., Müller, T., Niedermeier, N., Achterberg, E. P., Patey, M. D., Kozlova, E. A.,
776 Heimann, M., Heard, D. E., Plane, J. M. C., Mahajan, A., Oetjen, H., Ingham, T., Stone, D., Whalley, L.
777 K., Evans, M. J., Pilling, M. J., Leigh, R. J., Monks, P. S., Karunaharan, A., Vaughan, S., Arnold, S. R.,
778 Tschritter, J., Pöhler, D., Friess, U., Holla, R., Mendes, L. M., Lopez, H., Faria, B., Manning, A. J., and
779 Wallace, D. W. R.: Seasonal characteristics of tropical marine boundary layer air measured at the
780 Cape Verde Atmospheric Observatory, Journal of Atmospheric Chemistry, 67, 87-140,
781 10.1007/s10874-011-9206-1, 2010.

782 Chin, W. C., Orellana, M. V., and Verdugo, P.: Spontaneous assembly of marine dissolved
783 organic matter into polymer gels, Nature, 391, 568-572, 10.1038/35345, 1998.

784 Creamean, J. M., Cross, J. N., Pickart, R., McRaven, L., Lin, P., Pacini, A., Hanlon, R., Schmale, D.
785 G., Cenicerros, J., Aydell, T., Colombi, N., Bolger, E., and DeMott, P. J.: Ice Nucleating Particles Carried
786 From Below a Phytoplankton Bloom to the Arctic Atmosphere, Geophysical Research Letters, 46,
787 8572-8581, 10.1029/2019gl083039, 2019.

788 de Leeuw, G., Andreas, E. L., Anguelova, M. D., Fairall, C. W., Lewis, E. R., O'Dowd, C., Schulz,
789 M., and Schwartz, S. E.: Production Flux of Sea Spray Aerosol, Reviews of Geophysics, 49,
790 10.1029/2010rg000349, 2011.

791 Decho, A. W., and Gutierrez, T.: Microbial Extracellular Polymeric Substances (EPSs) in Ocean
792 Systems, Frontiers in Microbiology, 8, 10.3389/fmicb.2017.00922, 2017.

793 Deguillaume, L., and al., e.: Biological Activity in Clouds: From the Laboratory to the Model, in:
794 Air Pollution Modeling and its Application XXVI. ITM 2018., edited by: Mensink C., G. W., Hakami A. ,
795 pringer Proceedings in Complexity. Springer, Cham, 2020.

796 DeMott, P. J., Mason, R. H., McCluskey, C. S., Hill, T. C. J., Perkins, R. J., Desyaterik, Y., Bertram,
797 A. K., Trueblood, J. V., Grassian, V. H., Qiu, Y. Q., Molinero, V., Tobo, Y., Sultana, C. M., Lee, C., and
798 Prather, K. A.: Ice nucleation by particles containing long-chain fatty acids of relevance to freezing by
799 sea spray aerosols, Environmental Science-Processes & Impacts, 20, 1559-1569,
800 10.1039/c8em00386f, 2018.

801 Demoz, B. B., Collett, J. L., and Daube, B. C.: On the Caltech Active Strand Cloudwater
802 Collectors, Atmos Res, 41, 47-62, Doi 10.1016/0169-8095(95)00044-5, 1996.

803 Engel, A., Goldthwait, S., Passow, U., and Alldredge, A.: Temporal decoupling of carbon and
804 nitrogen dynamics in a mesocosm diatom bloom, Limnology and Oceanography, 47, 753-761,
805 10.4319/lo.2002.47.3.0753, 2002.

806 Engel, A., Delille, B., Jacquet, S., Riebesell, U., Rochelle-Newall, E., Terbruggen, A., and
807 Zondervan, I.: Transparent exopolymer particles and dissolved organic carbon production by
808 *Emiliana huxleyi* exposed to different CO₂ concentrations: a mesocosm experiment, *Aquatic*
809 *Microbial Ecology*, 34, 93-104, 10.3354/ame034093, 2004.

810 Engel, A.: Determination of Marine Gel Particles in: Practical guidelines for the analysis of
811 seawater, edited by: [u.a.], O. W. B. R., CRC Press, 2009.

812 Engel, A., Borchard, C., Loginova, A., Meyer, J., Hauss, H., and Kiko, R.: Effects of varied nitrate
813 and phosphate supply on polysaccharidic and proteinaceous gel particle production during tropical
814 phytoplankton bloom experiments, *Biogeosciences*, 12, 5647-5665, 10.5194/bg-12-5647-2015, 2015.

815 Engel, A., Endres, S., Galgani, L., and Schartau, M.: Marvelous Marine Microgels: On the
816 Distribution and Impact of Gel-Like Particles in the Oceanic Water-Column, *Frontiers in Marine*
817 *Science*, 7, 10.3389/fmars.2020.00405, 2020.

818 Ervens, B., and Amato, P.: The global impact of bacterial processes on carbon mass,
819 *Atmospheric Chemistry and Physics*, 20, 1777-1794, 10.5194/acp-20-1777-2020, 2020.

820 Facchini, M. C., Rinaldi, M., Decesari, S., Carbone, C., Finessi, E., Mircea, M., Fuzzi, S., Ceburnis,
821 D., Flanagan, R., Nilsson, E. D., de Leeuw, G., Martino, M., Woeltjen, J., and O'Dowd, C. D.: Primary
822 submicron marine aerosol dominated by insoluble organic colloids and aggregates, *Geophysical*
823 *Research Letters*, 35, 10.1029/2008gl034210, 2008.

824 Fomba, K. W., Müller, K., van Pinxteren, D., and Herrmann, H.: Aerosol size-resolved trace
825 metal composition in remote northern tropical Atlantic marine environment: case study Cape Verde
826 islands, *Atmospheric Chemistry and Physics*, 13, 4801-4814, 10.5194/acp-13-4801-2013, 2013.

827 Fomba, K. W., Mueller, K., van Pinxteren, D., Poulain, L., van Pinxteren, M., and Herrmann, H.:
828 Long-term chemical characterization of tropical and marine aerosols at the Cape Verde Atmospheric
829 Observatory (CVAO) from 2007 to 2011, *Atmospheric Chemistry and Physics*, 14, 8883-8904,
830 10.5194/acp-14-8883-2014, 2014.

831 Gao, Q., Leck, C., Rauschenberg, C., and Matrai, P. A.: On the chemical dynamics of
832 extracellular polysaccharides in the high Arctic surface microlayer, *Ocean Sci.*, 8, 401-418,
833 10.5194/os-8-401-2012, 2012.

834 Gong, X. D., Wex, H., van Pinxteren, M., Triesch, N., Fomba, K. W., Lubitz, J., Stolle, C.,
835 Robinson, T. B., Muller, T., Herrmann, H., and Stratmann, F.: Characterization of aerosol particles at
836 Cabo Verde close to sea level and at the cloud level - Part 2: Ice-nucleating particles in air, cloud and
837 seawater, *Atmospheric Chemistry and Physics*, 20, 1451-1468, 10.5194/acp-20-1451-2020, 2020a.

838 Gong, X. D., Wex, H., Voigtlander, J., Fomba, K. W., Weinhold, K., van Pinxteren, M., Henning,
839 S., Muller, T., Herrmann, H., and Stratmann, F.: Characterization of aerosol particles at Cabo Verde
840 close to sea level and at the cloud level - Part 1: Particle number size distribution, cloud condensation
841 nuclei and their origins, *Atmospheric Chemistry and Physics*, 20, 1431-1449, 10.5194/acp-20-1431-
842 2020, 2020b.

843 Hartmann, M., Adachi, K., Eppers, O., Haas, C., Herber, A., Holzinger, R., Hunerbein, A., Jakel,
844 E., Jentsch, C., van Pinxteren, M., Wex, H., Willmes, S., and Stratmann, F.: Wintertime Airborne
845 Measurements of Ice Nucleating Particles in the High Arctic: A Hint to a Marine, Biogenic Source for
846 Ice Nucleating Particles, *Geophysical Research Letters*, 47, 10.1029/2020gl087770, 2020.

847 Hoffman, E. J., and Duce, R. A.: Factors influencing organic-carbon content of marine aerosols -
848 Laboratory study, *J. Geophys. Res.*, 81, 3667–3670, 1976.

849 Jaber, S., Joly, M., Brissy, M., Lereboure, M., Khaled, A., Ervens, B., and Delort, A. M.: Biotic
850 and abiotic transformation of amino acids in cloud water: experimental studies and atmospheric
851 implications, *Biogeosciences*, 18, 1067-1080, 10.5194/bg-18-1067-2021, 2021.

852 Keene, W. C., Maring, H., Maben, J. R., Kieber, D. J., Pszenny, A. A. P., Dahl, E. E., Izaguirre, M.
853 A., Davis, A. J., Long, M. S., Zhou, X., Smoydzin, L., and Sander, R.: Chemical and physical
854 characteristics of nascent aerosols produced by bursting bubbles at a model air-sea interface, *Journal*
855 *of Geophysical Research-Atmospheres*, 112, 10.1029/2007jd008464, 2007.

856 Khaled, A., Zhang, M. H., Amato, P., Delort, A. M., and Ervens, B.: Biodegradation by bacteria in
857 clouds: an underestimated sink for some organics in the atmospheric multiphase system,
858 *Atmospheric Chemistry and Physics*, 21, 3123-3141, 10.5194/acp-21-3123-2021, 2021.

859 Kuznetsova, M., Lee, C., and Aller, J.: Characterization of the proteinaceous matter in marine
860 aerosols, *Marine Chemistry*, 96, 359-377, 10.1016/j.marchem.2005.03.007, 2005.

861 Leck, C., and Bigg, E. K.: Source and evolution of the marine aerosol - A new perspective,
862 *Geophysical Research Letters*, 32, 10.1029/2005gl023651, 2005a.

863 Leck, C., and Bigg, E. K.: Biogenic particles in the surface microlayer and overlying atmosphere
864 in the central Arctic Ocean during summer, *Tellus Ser. B-Chem. Phys. Meteorol.*, 57, 305-316,
865 10.1111/j.1600-0889.2005.00148.x, 2005b.

866 Leck, C., Gao, Q., Rad, F. M., and Nilsson, U.: Size-resolved atmospheric particulate
867 polysaccharides in the high summer Arctic, *Atmospheric Chemistry and Physics*, 13, 12573-12588,
868 10.5194/acp-13-12573-2013, 2013.

869 Lewandowska, A. U., and Falkowska, L. M.: Sea salt in aerosols over the southern Baltic. Part 1.
870 The generation and transportation of marine particles, *Oceanologia*, 55, 279-298, 10.5697/oc.55-
871 2.279, 2013.

872 Lewandowska, A. U., Sliwinska-Wilczewska, S., and Wozniczka, D.: Identification of
873 cyanobacteria and microalgae in aerosols of various sizes in the air over the Southern Baltic Sea,
874 *Marine Pollution Bulletin*, 125, 30-38, 10.1016/j.marpolbul.2017.07.064, 2017.

875 Liss, P. S., and Johnson, M. T.: *Ocean-Atmosphere Interactions of Gases and Particles*, Springer,
876 2014.

877 Logan, B. E., Passow, U., Alldredge, A. L., Grossartt, H.-P., and Simont, M.: Rapid formation and
878 sedimentation of large aggregates is predictable from coagulation rates (half-lives) of transparent
879 exopolymer particles (TEP), *Deep Sea Research Part II: Topical Studies in Oceanography*, 42, 203-214,
880 [https://doi.org/10.1016/0967-0645\(95\)00012-F](https://doi.org/10.1016/0967-0645(95)00012-F), 1995.

881 Louis, J., Pedrotti, M. L., Gazeau, F., and Guieu, C.: Experimental evidence of formation of
882 Transparent Exopolymer Particles (TEP) and POC export provoked by dust addition under current and
883 high pCO₂ conditions, *Plos One*, 12, 10.1371/journal.pone.0171980, 2017.

884 Madry, W. L., Toon, O. B., and O'Dowd, C. D.: Modeled optical thickness of sea-salt aerosol,
885 *Journal of Geophysical Research-Atmospheres*, 116, 10.1029/2010jd014691, 2011.

886 Maki, T., Lee, K. C., Kawai, K., Onishi, K., Hong, C. S., Kurosaki, Y., Shinoda, M., Kai, K., Iwasaka,
887 Y., Archer, S. D. J., Lacap-Bugler, D. C., Hasegawa, H., and Pointing, S. B.: Aeolian Dispersal of Bacteria
888 Associated With Desert Dust and Anthropogenic Particles Over Continental and Oceanic Surfaces,
889 *Journal of Geophysical Research-Atmospheres*, 124, 5579-5588, 10.1029/2018jd029597, 2019.

890 Malfatti, F., Lee, C., Tinta, T., Pendergraft, M. A., Celussi, M., Zhou, Y. Y., Sultana, C. M., Rotter,
891 A., Axson, J. L., Collins, D. B., Santander, M. V., Morales, A. L. A., Aluwihare, L. I., Riemer, N., Grassian,
892 V. H., Azam, F., and Prather, K. A.: Detection of Active Microbial Enzymes in Nascent Sea Spray
893 Aerosol: Implications for Atmospheric Chemistry and Climate, *Environmental Science & Technology*
894 *Letters*, 6, 171-177, 10.1021/acs.estlett.8b00699, 2019.

895 Mari, X., Passow, U., Migon, C., Burd, A. B., and Legendre, L.: Transparent exopolymer
896 particles: Effects on carbon cycling in the ocean, *Progress in Oceanography*, 151, 13-37,
897 10.1016/j.pocean.2016.11.002, 2017.

898 Marone, A., Kane, C. T., Mbengue, M., Jenkins, G. S., Niang, D. N., Drame, M. S., and Gernand,
899 J. M.: Characterization of Bacteria on Aerosols From Dust Events in Dakar, Senegal, West Africa,
900 *Geohealth*, 4, 10.1029/2019gh000216, 2020.

901 Matulova, M., Husarova, S., Capek, P., Sancelme, M., and Delort, A. M.: Biotransformation of
902 Various Saccharides and Production of Exopolymeric Substances by Cloud-Borne *Bacillus* sp 3B6,
903 *Environmental Science & Technology*, 48, 14238-14247, 10.1021/es501350s, 2014.

904 McCluskey, C. S., Hill, T. C. J., Humphries, R. S., Rauker, A. M., Moreau, S., Strutton, P. G.,
905 Chambers, S. D., Williams, A. G., McRobert, I., Ward, J., Keywood, M. D., Harnwell, J., Ponsonby, W.,
906 Loh, Z. M., Krummel, P. B., Protat, A., Kreidenweis, S. M., and DeMott, P. J.: Observations of Ice
907 Nucleating Particles Over Southern Ocean Waters, *Geophysical Research Letters*, 45, 11989-11997,
908 10.1029/2018gl079981, 2018a.

909 McCluskey, C. S., Ovadnevaite, J., Rinaldi, M., Atkinson, J., Belosi, F., Ceburnis, D., Marullo, S.,
910 Hill, T. C. J., Lohmann, U., Kanji, Z. A., O'Dowd, C., Kreidenweis, S. M., and DeMott, P. J.: Marine and
911 Terrestrial Organic Ice-Nucleating Particles in Pristine Marine to Continentally Influenced Northeast
912 Atlantic Air Masses, *Journal of Geophysical Research-Atmospheres*, 123, 6196-6212,
913 10.1029/2017jd028033, 2018b.

914 Mimura, T., and Romano, J. C.: Muramin acid measurements for bacterial investigations in
915 marine environments by high-pressure-liquid-chromatography, *Applied and Environmental*
916 *Microbiology*, 50, 229-237, 10.1128/aem.50.2.229-237.1985, 1985.

917 Niedermeier, N., Held, A., Müller, T., Heinold, B., Schepanski, K., Tegen, I., Kandler, K., Ebert,
918 M., Weinbruch, S., Read, K., Lee, J., Fomba, K. W., Müller, K., Herrmann, H., and Wiedensohler, A.:
919 Mass deposition fluxes of Saharan mineral dust to the tropical northeast Atlantic Ocean: an
920 intercomparison of methods, *Atmos. Chem. Phys.*, 14, 2245-2266, 10.5194/acp-14-2245-2014, 2014.

921 O'Dowd, C. D., Facchini, M. C., Cavalli, F., Ceburnis, D., Mircea, M., Decesari, S., Fuzzi, S., Yoon,
922 Y. J., and Putaud, J. P.: Biogenically driven organic contribution to marine aerosol, *Nature*, 431, 676-
923 680, Doi 10.1038/Nature02959, 2004.

924 Orellana, M. V., and Verdugo, P.: Ultraviolet radiation blocks the organic carbon exchange
925 between the dissolved phase and the gel phase in the ocean, *Limnology and Oceanography*, 48,
926 1618-1623, 10.4319/lb.2003.48.4.1618, 2003.

927 Orellana, M. V., Matrai, P. A., Leck, C., Rauschenberg, C. D., Lee, A. M., and Coz, E.: Marine
928 microgels as a source of cloud condensation nuclei in the high Arctic, *Proceedings of the National*
929 *Academy of Sciences of the United States of America*, 108, 13612-13617, 10.1073/pnas.1102457108,
930 2011.

931 Ovadnevaite, J., O'Dowd, C., Dall'Osto, M., Ceburnis, D., Worsnop, D. R., and Berresheim, H.:
932 Detecting high contributions of primary organic matter to marine aerosol: A case study, *Geophysical*
933 *Research Letters*, 38, 10.1029/2010gl046083, 2011.

934 Pandey, R., Usui, K., Livingstone, R. A., Fischer, S. A., Pfaendtner, J., Backus, E. H. G., Nagata, Y.,
935 Frohlich-Nowoisky, J., Schmuser, L., Mauri, S., Scheel, J. F., Knopf, D. A., Poschl, U., Bonn, M., and
936 Weidner, T.: Ice-nucleating bacteria control the order and dynamics of interfacial water, *Science*
937 *Advances*, 2, 10.1126/sciadv.1501630, 2016.

938 Passow, U., and Alldredge, A.: A dye-binding assay for the spectrophotometric measurement of
939 transparent exopolymer particles (TEP), *Limnology and Oceanography*, 40, 10, 1995.

940 Passow, U.: Formation of transparent exopolymer particles, TEP, from dissolved precursor
941 material, *Marine Ecology Progress Series*, 192, 1-11, 10.3354/meps192001, 2000.

942 Passow, U.: Production of transparent exopolymer particles (TEP) by phyto- and
943 bacterioplankton, *Marine Ecology-progress Series - MAR ECOL-PROGR SER*, 236, 1-12,
944 10.3354/meps236001, 2002a.

945 Passow, U.: Transparent exopolymer particles (TEP) in aquatic environments, *Progress in*
946 *Oceanography*, 55, 287-333, 10.1016/s0079-6611(02)00138-6, 2002b.

947 Pummer, B. G., Budke, C., Augustin-Bauditz, S., Niedermeier, D., Felgitsch, L., Kampf, C. J.,
948 Huber, R. G., Liedl, K. R., Loerting, T., Moschen, T., Schauperl, M., Tollinger, M., Morris, C. E., Wex, H.,
949 Grothe, H., Poschl, U., Koop, T., and Frohlich-Nowoisky, J.: Ice nucleation by water-soluble
950 macromolecules, *Atmospheric Chemistry and Physics*, 15, 4077-4091, 10.5194/acp-15-4077-2015,
951 2015.

952 Quinn, P. K., Collins, D. B., Grassian, V. H., Prather, K. A., and Bates, T. S.: Chemistry and
953 Related Properties of Freshly Emitted Sea Spray Aerosol, *Chemical Reviews*, 115, 4383-4399,
954 10.1021/cr5007139, 2015.

955 Rastelli, E., Corinaldesi, C., Dell'Anno, A., Lo Martire, M., Greco, S., Facchini, M. C., Rinaldi, M.,
956 O'Dowd, C., Ceburnis, D., and Danovaro, R.: Transfer of labile organic matter and microbes from the
957 ocean surface to the marine aerosol: an experimental approach, *Scientific Reports*, 7,
958 10.1038/s41598-017-10563-z, 2017.

959 Robinson, T. B., Stolle, C., and Wurl, O.: Depth is relative: the importance of depth for
960 transparent exopolymer particles in the near-surface environment, *Ocean Science*, 15, 1653-1666,
961 10.5194/os-15-1653-2019, 2019a.

962 Robinson, T. B., Wurl, O., Bahlmann, E., Juergens, K., and Stolle, C.: Rising bubbles enhance the
963 gelatinous nature of the air-sea interface, *Limnology and Oceanography*, 64, 2358-2372,
964 10.1002/lno.11188, 2019b.

965 Sander, R., Keene, W. C., Pszenny, A. A. P., Arimoto, R., Ayers, G. P., Baboukas, E., Caine, J. M.,
966 Crutzen, P. J., Duce, R. A., Honninger, G., Huebert, B. J., Maenhaut, W., Mihalopoulos, N., Turekian, V.

967 C., and Van Dingenen, R.: Inorganic bromine in the marine boundary layer: a critical review,
968 *Atmospheric Chemistry and Physics*, 3, 1301-1336, 2003.

969 Schmitt-Kopplin, P., Liger-Belair, G., Koch, B. P., Flerus, R., Kattner, G., Harir, M., Kanawati, B.,
970 Lucio, M., Tziotis, D., Hertkorn, N., and Gebefuegi, I.: Dissolved organic matter in sea spray: a transfer
971 study from marine surface water to aerosols, *Biogeosciences*, 9, 1571-1582, 10.5194/bg-9-1571-
972 2012, 2012.

973 Schuster, S., and Herndl, G. J.: Formation and significance of transparent exopolymeric
974 particles in the northern adriatic sea *Marine Ecology Progress Series*, 124, 227-236,
975 10.3354/meps124227, 1995.

976 Sellegri, K., Nicosia, A., Freney, E., Uitz, J., Thyssen, M., Grégori, G., Engel, A., Zäncker, B.,
977 Haëntjens, N., Mas, S., Picard, D., Saint-Macary, A., Peltola, M., Rose, C., Trueblood, J., Lefevre, D.,
978 D'Anna, B., Desboeufs, K., Meskhidze, N., Guieu, C., and Law, C. S.: Surface ocean microbiota
979 determine cloud precursors, *Scientific Reports*, 11, 281, 10.1038/s41598-020-78097-5, 2021.

980 Sharma, N. K., Rai, A. K., Singh, S., and Brown, R. M.: Airborne algae: Their present status and
981 relevance, *Journal of Phycology*, 43, 615-627, 10.1111/j.1529-8817.2007.00373.x, 2007.

982 Triesch, N., van Pinxteren, M., Engel, A., and Herrmann, H.: Concerted measurements of free
983 amino acids at the Cape Verde Islands: High enrichments in submicron sea spray aerosol particles
984 and cloud droplets, *Atmos. Chem. Phys.*, 21, 163–181, 2021a.

985 Triesch, N., van Pinxteren, M., Frka, S., Stolle, C., Spranger, T., Hoffmann, E. H., Gong, X., Wex,
986 H., Schulz-Bull, D., Gašparović, B., and Herrmann, H.: Concerted measurements of lipids in seawater
987 and on submicrometer aerosol particles at the Cabo Verde islands: biogenic sources, selective
988 transfer and high enrichments, *Atmos. Chem. Phys.*, 21, 4267-4283, 10.5194/acp-21-4267-2021,
989 2021b.

990 Turekian, K. K.: *Oceans (Foundations of Earth Science)*, Prentice Hall; 1st Edition, 1968.

991 Uetake, J., Hill, T. C. J., Moore, K. A., DeMott, P. J., Protat, A., and Kreidenweis, S. M.: Airborne
992 bacteria confirm the pristine nature of the Southern Ocean boundary layer, *Proceedings of the*
993 *National Academy of Sciences of the United States of America*, 117, 13275-13282,
994 10.1073/pnas.2000134117, 2020.

995 van Pinxteren, M., Barthel, S., Fomba, K., Müller, K., von Tümpling, W., and Herrmann, H.: The
996 influence of environmental drivers on the enrichment of organic carbon in the sea surface microlayer
997 and in submicron aerosol particles – measurements from the Atlantic Ocean, *Elem Sci Anth*, 5,
998 <https://doi.org/10.1525/elementa.225>, 2017.

999 van Pinxteren, M., Fomba, K. W., Triesch, N., Stolle, C., Wurl, O., Bahlmann, E., Gong, X. D.,
1000 Voigtlander, J., Wex, H., Robinson, T. B., Barthel, S., Zeppenfeld, S., Hoffmann, E. H., Roveretto, M., Li,
1001 C. L., Grosselin, B., Daele, V., Senf, F., van Pinxteren, D., Manzi, M., Zabalegui, N., Frka, S., Gasparovic,
1002 B., Pereira, R., Li, T., Wen, L., Li, J. R., Zhu, C., Chen, H., Chen, J. M., Fiedler, B., Von Tümpling, W.,
1003 Read, K. A., Punjabi, S., Lewis, A. C., Hopkins, J. R., Carpenter, L. J., Peeken, I., Rixen, T., Schulz-Bull,
1004 D., Monge, M. E., Mellouki, A., George, C., Stratmann, F., and Herrmann, H.: Marine organic matter in
1005 the remote environment of the Cape Verde islands - an introduction and overview to the
1006 MarParCloud campaign, *Atmospheric Chemistry and Physics*, 20, 6921-6951, 10.5194/acp-20-6921-
1007 2020, 2020.

1008 Verdugo, P., Alldredge, A. L., Azam, F., Kirchman, D. L., Passow, U., and Santschi, P. H.: The
1009 oceanic gel phase: a bridge in the DOM–POM continuum, *Marine Chemistry*, 92, 67-85, 2004.

1010 Villacorte, L. O., Ekowati, Y., Calix-Ponce, H. N., Schippers, J. C., Amy, G. L., and Kennedy, M. D.:
1011 Improved method for measuring transparent exopolymer particles (TEP) and their precursors in fresh
1012 and saline water, *Water Research*, 70, 300-312, 10.1016/j.watres.2014.12.012, 2015.

1013 Wiedensohler, A., Birmili, W., Nowak, A., Sonntag, A., Weinhold, K., Merkel, M., Wehner, B.,
1014 Tuch, T., Pfeifer, S., Fiebig, M., Fjaraa, A. M., Asmi, E., Sellegri, K., Depuy, R., Venzac, H., Villani, P., Laj,
1015 P., Aalto, P., Ogren, J. A., Swietlicki, E., Williams, P., Roldin, P., Quincey, P., Hüglin, C., Fierz-
1016 Schmidhauser, R., Gysel, M., Weingartner, E., Riccobono, F., Santos, S., Gruning, C., Faloon, K.,
1017 Beddows, D., Harrison, R. M., Monahan, C., Jennings, S. G., O'Dowd, C. D., Marinoni, A., Horn, H. G.,
1018 Keck, L., Jiang, J., Scheckman, J., McMurry, P. H., Deng, Z., Zhao, C. S., Moerman, M., Henzing, B., de
1019 Leeuw, G., Loschau, G., and Bastian, S.: Mobility particle size spectrometers: harmonization of
1020 technical standards and data structure to facilitate high quality long-term observations of
1021 atmospheric particle number size distributions, *Atmospheric Measurement Techniques*, 5, 657-685,
1022 10.5194/amt-5-657-2012, 2012.

1023 Wilson, T. W., Ladino, L. A., Alpert, P. A., Breckels, M. N., Brooks, I. M., Browse, J., Burrows, S.
1024 M., Carslaw, K. S., Huffman, J. A., Judd, C., Kilitau, W. P., Mason, R. H., McFiggans, G., Miller, L. A.,
1025 Najera, J. J., Polishchuk, E., Rae, S., Schiller, C. L., Si, M., Temprado, J. V., Whale, T. F., Wong, J. P. S.,
1026 Wurl, O., Yakobi-Hancock, J. D., Abbatt, J. P. D., Aller, J. Y., Bertram, A. K., Knopf, D. A., and Murray, B.
1027 J.: A marine biogenic source of atmospheric ice-nucleating particles, *Nature*, 525, 234-+,
1028 10.1038/nature14986, 2015.

1029 Wiśniewska, K., Lewandowska, A. U., and Śliwińska-Wilczewska, S.: The importance of
1030 cyanobacteria and microalgae present in aerosols to human health and the environment - Review
1031 study, *Environment International*, 131, 10.1016/j.envint.2019.104964, 2019.

1032 Wiśniewska, K. A., Śliwińska-Wilczewska, S., and Lewandowska, A. U.: Airborne microalgal and
1033 cyanobacterial diversity and composition during rain events in the southern Baltic Sea region,
1034 *Scientific Reports*, 12, 2029, 10.1038/s41598-022-06107-9, 2022.

1035 Wurl, O., and Holmes, M.: The gelatinous nature of the sea-surface microlayer, *Marine*
1036 *Chemistry*, 110, 89-97, 10.1016/j.marchem.2008.02.009, 2008.

1037 Wurl, O., Miller, L., and Vagle, S.: Production and fate of transparent exopolymer particles in
1038 the ocean, *J. Geophys. Res.-Oceans*, 116, 10.1029/2011jc007342, 2011.

1039 Zäncker, B., Engel, A., and Cunliffe, M.: Bacterial communities associated with individual
1040 transparent exopolymer particles (TEP), *Journal of Plankton Research*, 41, 561-565,
1041 10.1093/plankt/fbz022, 2019.

1042 Zeppenfeld, S., van Pinxteren, M., Hartmann, M., Bracher, A., Stratmann, F., and Herrmann, H.:
1043 Glucose as a Potential Chemical Marker for Ice Nucleating Activity in Arctic Seawater and Melt Pond
1044 Samples, *Environmental Science & Technology*, 53, 8747-8756, 10.1021/acs.est.9b01469, 2019.

1045 Zeppenfeld, S., van Pinxteren, M., van Pinxteren, D., Wex, H., Berdalet, E., Vaqué, D., Dall'Osto,
1046 M., and Herrmann, H.: Aerosol Marine Primary Carbohydrates and Atmospheric Transformation in
1047 the Western Antarctic Peninsula, *ACS Earth Space Chem.*, 10.1021/acsearthspacechem.0c00351,
1048 2021.

1049 Zhang, M. H., Khaled, A., Amato, P., Delort, A. M., and Ervens, B.: Sensitivities to biological
1050 aerosol particle properties and ageing processes: potential implications for aerosol-cloud interactions
1051 and optical properties, *Atmospheric Chemistry and Physics*, 21, 3699-3724, 10.5194/acp-21-3699-
1052 2021, 2021.

1053

1054

1055

1056 **Caption of Figures:**

1057 **Figure 1:** Microscopic analysis of TEP from the cloud water sample “WW5” (sampling interval:
1058 28.09. 19:30 – 29.09. 7:30 local time). Blue particles are TEP, stained with Alcian Blue solution;
1059 brownish particles in the right picture are assumingly dust particles. The scale refers to 50 μm .
1060

1061 **Figure 2:** TEP number concentrations in the aerosol particles (red bars) and in the three cloud
1062 water samples (black-red squares). TEP concentrations were below the limit of detection
1063 (LOD) on 26th and 27th of September 2017. The backgrounds represent the dust classification
1064 according to the ambient dust concentrations (blue: dust < 5 $\mu\text{g m}^{-3}$ marine conditions; yellow:
1065 dust < 20 $\mu\text{g m}^{-3}$ (low dust); brown: dust < 60 $\mu\text{g m}^{-3}$ (moderate dust). From underlined dates
1066 (22.09 -> “TEP5” and 28.09.2017 -> “TEP10”) TEP number size distributions were measured.
1067

1068 **Figure 3:** Box and whisker plot of the TEP number concentrations (a) and the enrichment
1069 factors (b) in the ambient (n=18) and tank-generated (n=4) aerosol particles and in the cloud
1070 water samples (n=3), Each box encloses 50% of the data with the mean value represented as
1071 an open square and the median value represented as a line. The bottom of the box marks the
1072 25% limit of the data, while the top marks the 75% limit. The lines extending from the top and
1073 bottom of each box are the 5% and 95% percentiles within the data set, while the asterisks
1074 indicate the data points lying outside of this range (“outliers”).

1075 **Figure 4:** TEP number size distribution in the aerosol particles and cloud water in linear and
1076 logarithmic form; panels (a) and (b) show aerosol particle sample “TEP 5” (sampling start:
1077 22.09.2017), panels (c) and (d) show aerosol sample “TEP 10” (sampling start: 28.09.2017),
1078 panels (e) and (f) show cloud water sample “WW5” (sampling interval: 28.09. 19:30 – 29.09.
1079 7:30 local time. The lower limit of the resolution of the microscope was 16 μm^2 resulting in a
1080 particle diameter of 4.5 μm (assuming spherical particle). Each bar in a), c), and e) represents
1081 the summed up particle number concentrations (within 1.5 μm), e.g. the first column
1082 represents the summed up concentrations between 4.5 and 6 μm .

1083

1084 **Figure 5:** TEP number size distributions in the ocean surface water (sampling depth: 10 m)
1085 from the East Tropical North Atlantic (ETNA), averaged over three stations from Engel et al
1086 (2020). The data in this Figure show the size distribution between ~ 5 and ~ 30 μm , matching
1087 the investigated aerosol size range (**Fig. 4**). The whole size spectrum is shown in **Tab. S5**.
1088

1089 **Figure 6:** Relative contribution of the TEP number concentrations in the aerosol particles
1090 (left) and in the ocean surface water (right) regarding the identical size bins.

1091

1092 **Figure 7:** Correlations of TEP volume concentrations (size range: 5-10 μm) to chemical
1093 parameters (inorganic constituents PM10) and dust (PM10), as well as correlation of TEP
1094 number concentration and INP number concentrations. Inorganic constituents were
1095 measured with ion chromatography and dust concentrations were derived from PM10
1096 concentrations as reported elsewhere (Fomba et al., 2013;van Pinxteren et al., 2020).
1097 Measurements of INP number concentrations and error bars are explained in (Gong et al.,
1098 2020a)

1099

1100

1101

1102

1103

1104

1105

1106

1107

1108

1109

1110

1111

1112

1113

1114

1115

1116

1117

1118

1119

1120

1121

1122

1123

1124

1125

1126

1127

1128
 1129
 1130
 1131
 1132

Table 1. Overview of sampling locations, types and measurements

Sampling site	Campaign	Sample type	Coordinates	No. of samples	Measurements (Particle sizes)
CVAO	MarParCloud 2017	Ambient aerosol particles Inlet hight: 42 m a.s.l	16° 51.49' N, 24° 52.02' W	20 20	#TEP (TSP) Inorganic ions (PM ₁₀)
Mt- Verde	MarParCloud 2017	Ambient cloud water Inlet hight: 746 m a.s.l	16°52.11'N, 24°56.02'W	3	#TEP Inorganic ions
Plunging waterfall tank (operated at CVAO)	MarParCloud 2017	Tank-generated aerosol particles	16° 51.49' N, 24° 52.02' W	4	#TEP (TSP) Inorganic ions (TSP)
ETNA (Mauretanian upwelling)	M107 RV Meteor 2012	Ocean surface water	18.00/18.19'N -16.50/72.02'E	6	#TEP

1133
 1134
 1135
 1136
 1137

1138
1139
1140
1141
1142
1143
1144
1145
1146
1147
1148
1149
1150
1151
1152
1153
1154
1155

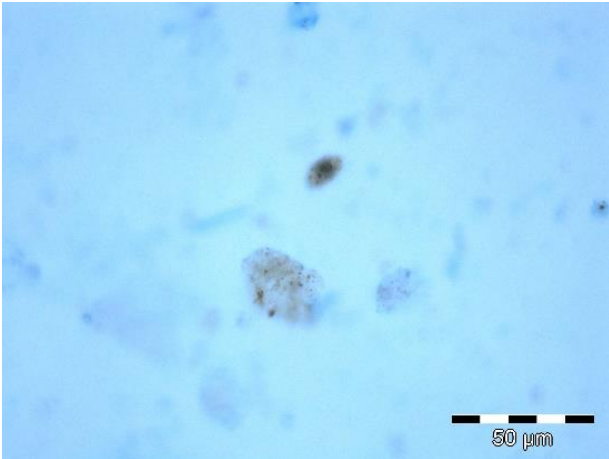
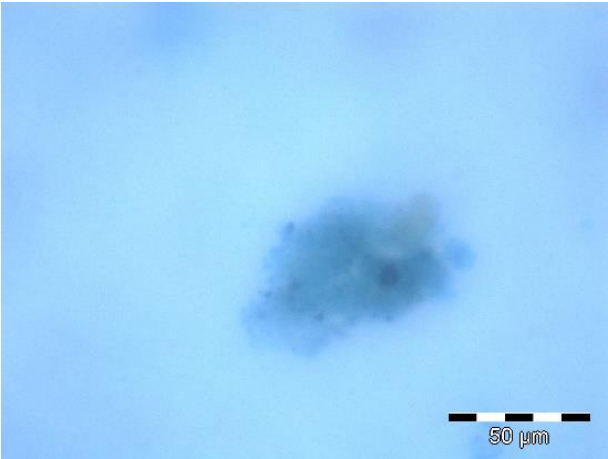


Figure 1

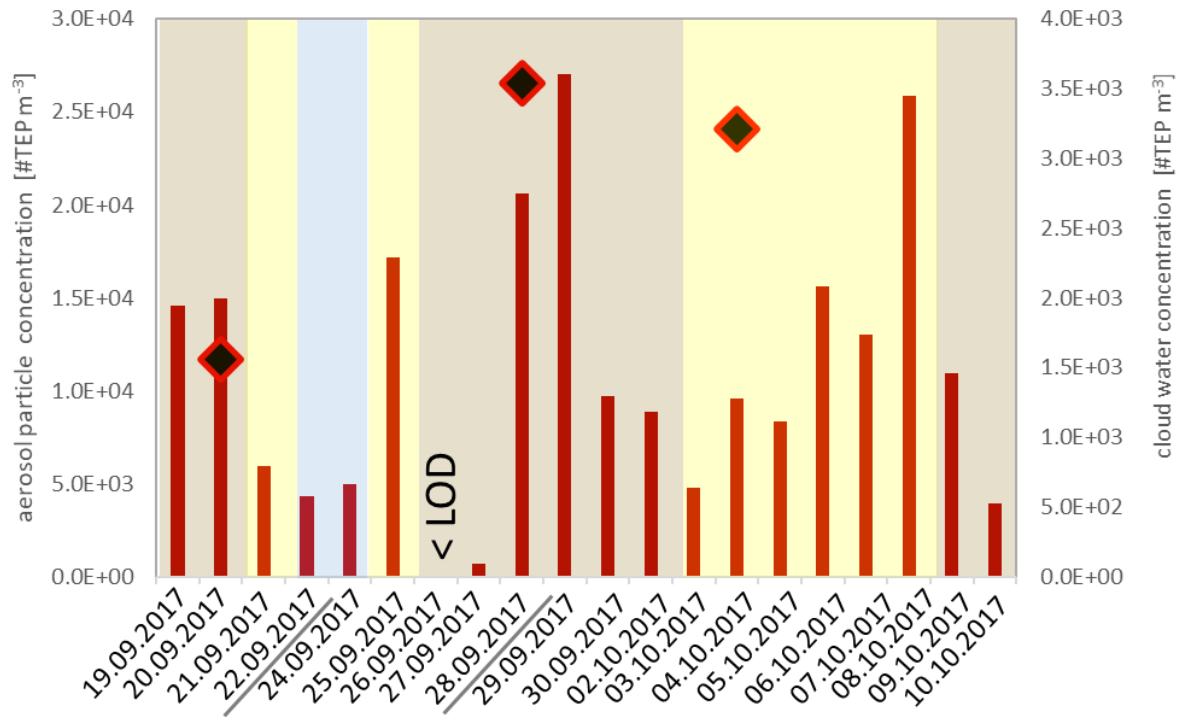


Figure 2

1156

1157

1158

1159

1160

1161

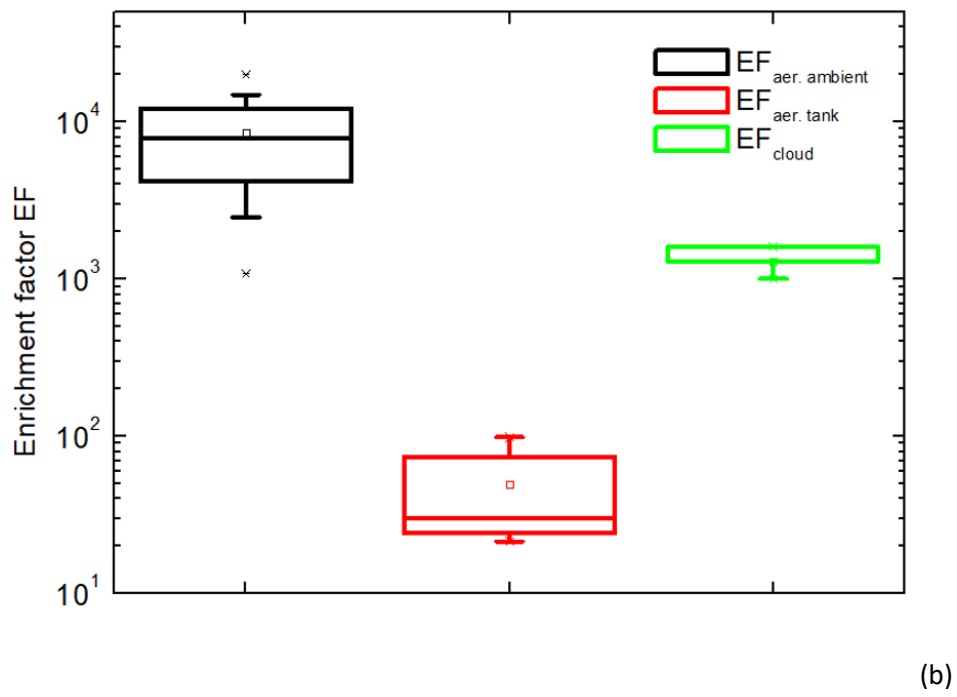
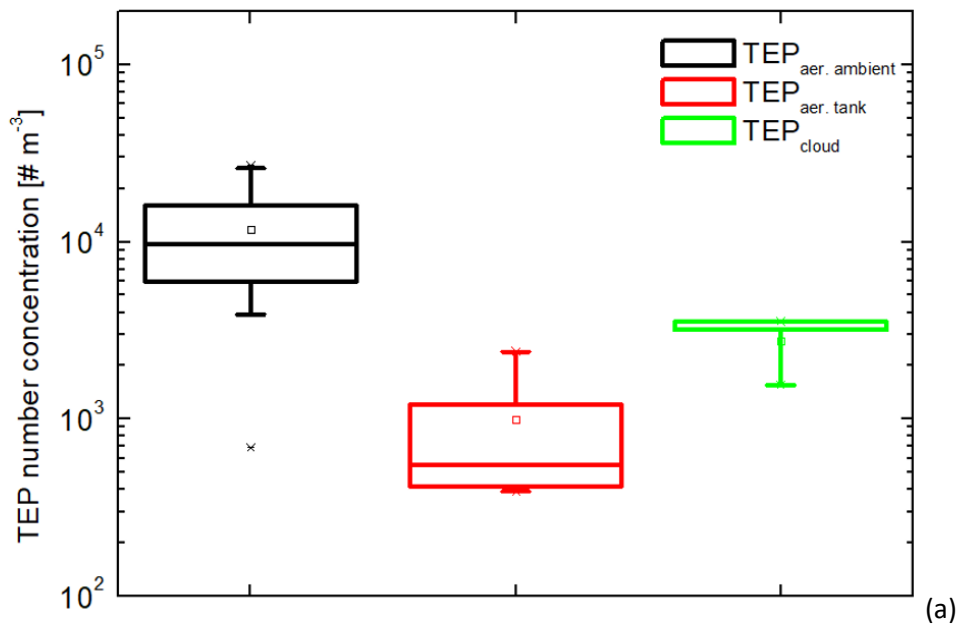
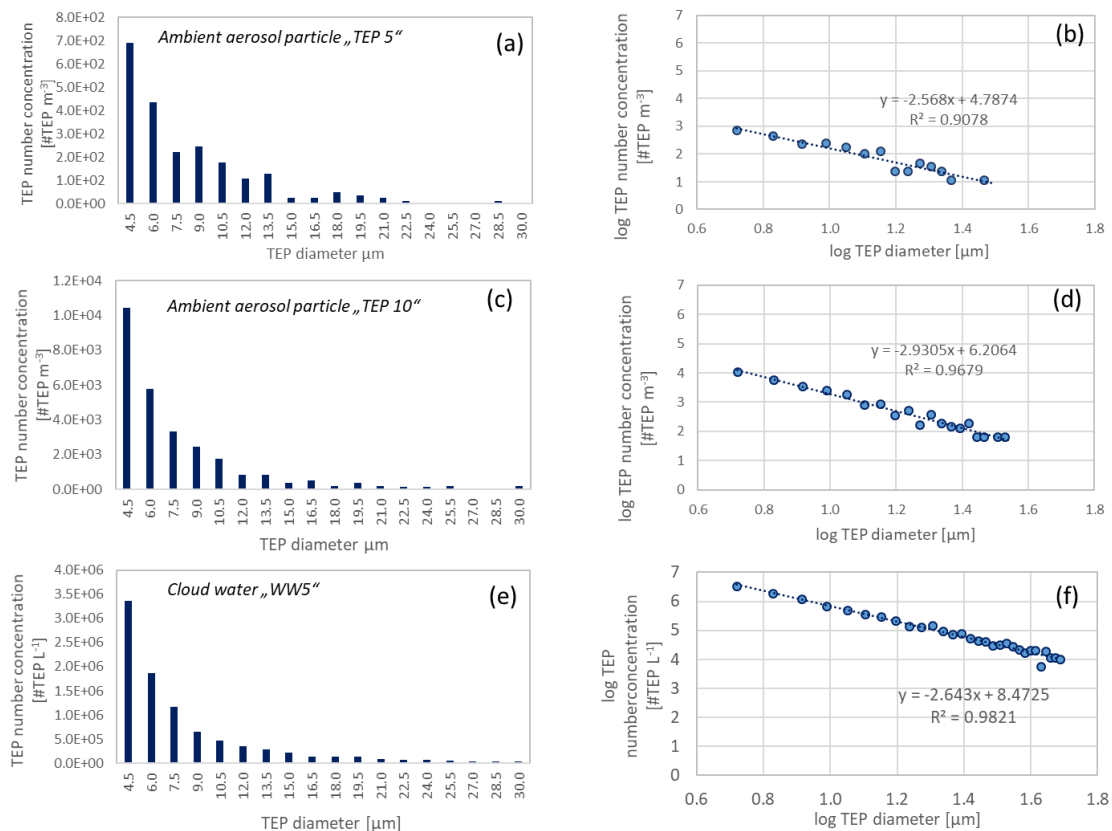


Figure 3

1178

1179



1180

1181

1182

1183

1184

1185

1186

1187

1188

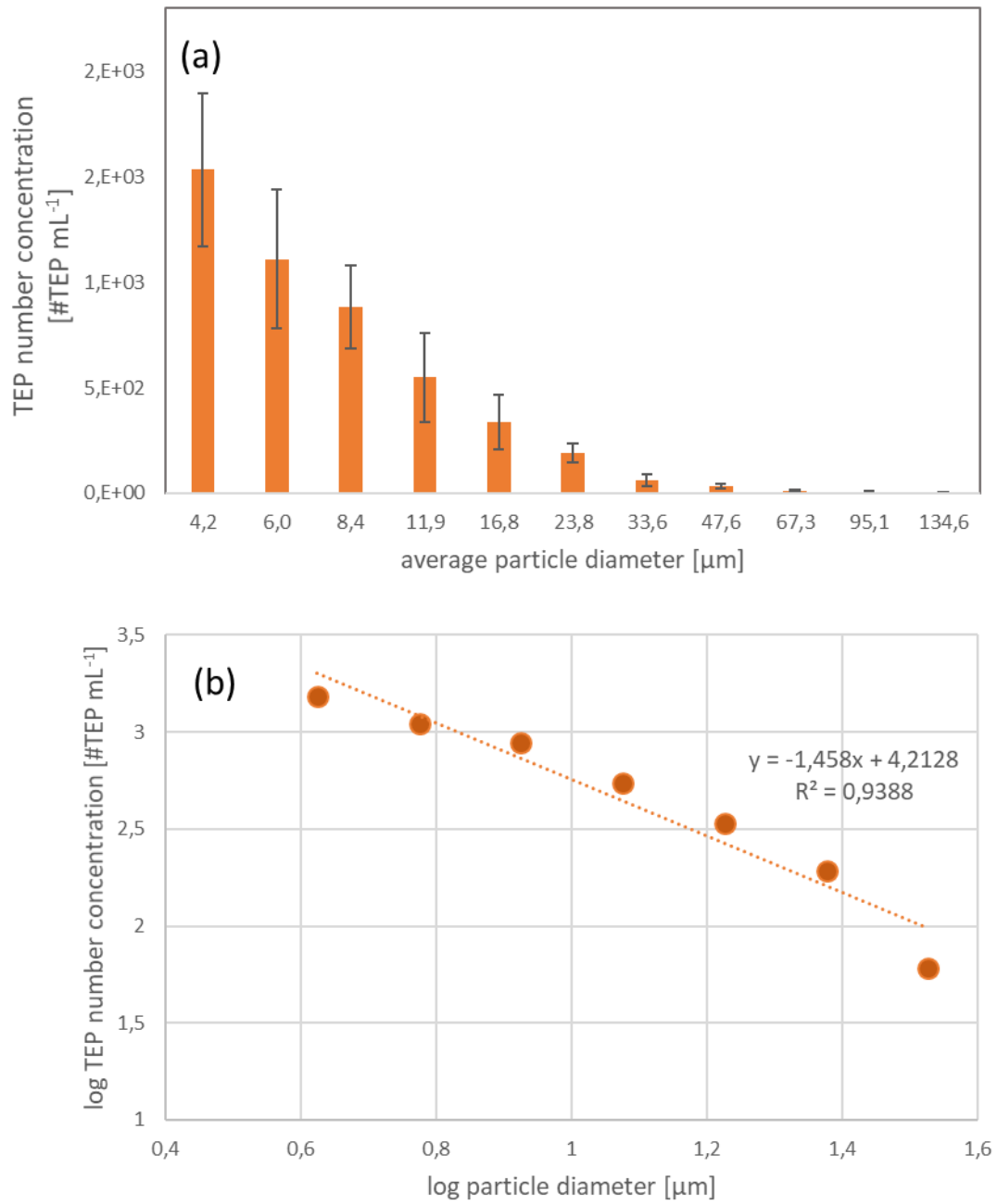
1189

1190

1191

Figure 4

1192



1193

1194

1195

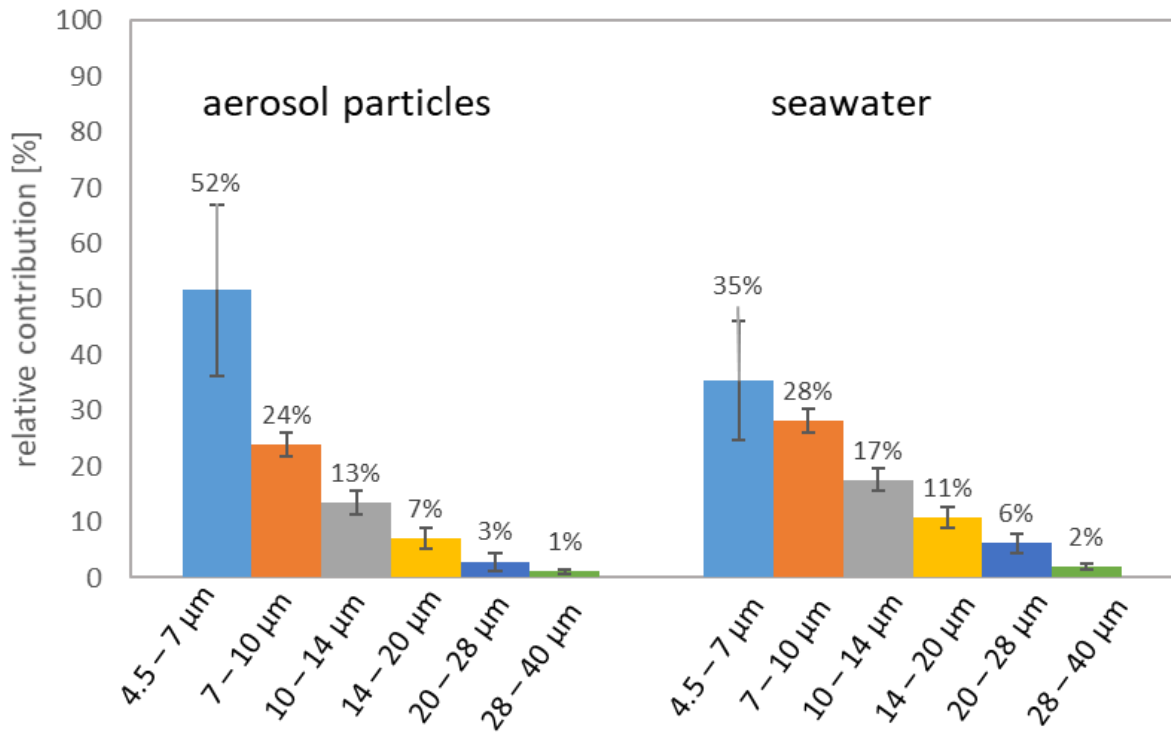
1196

1197

1198

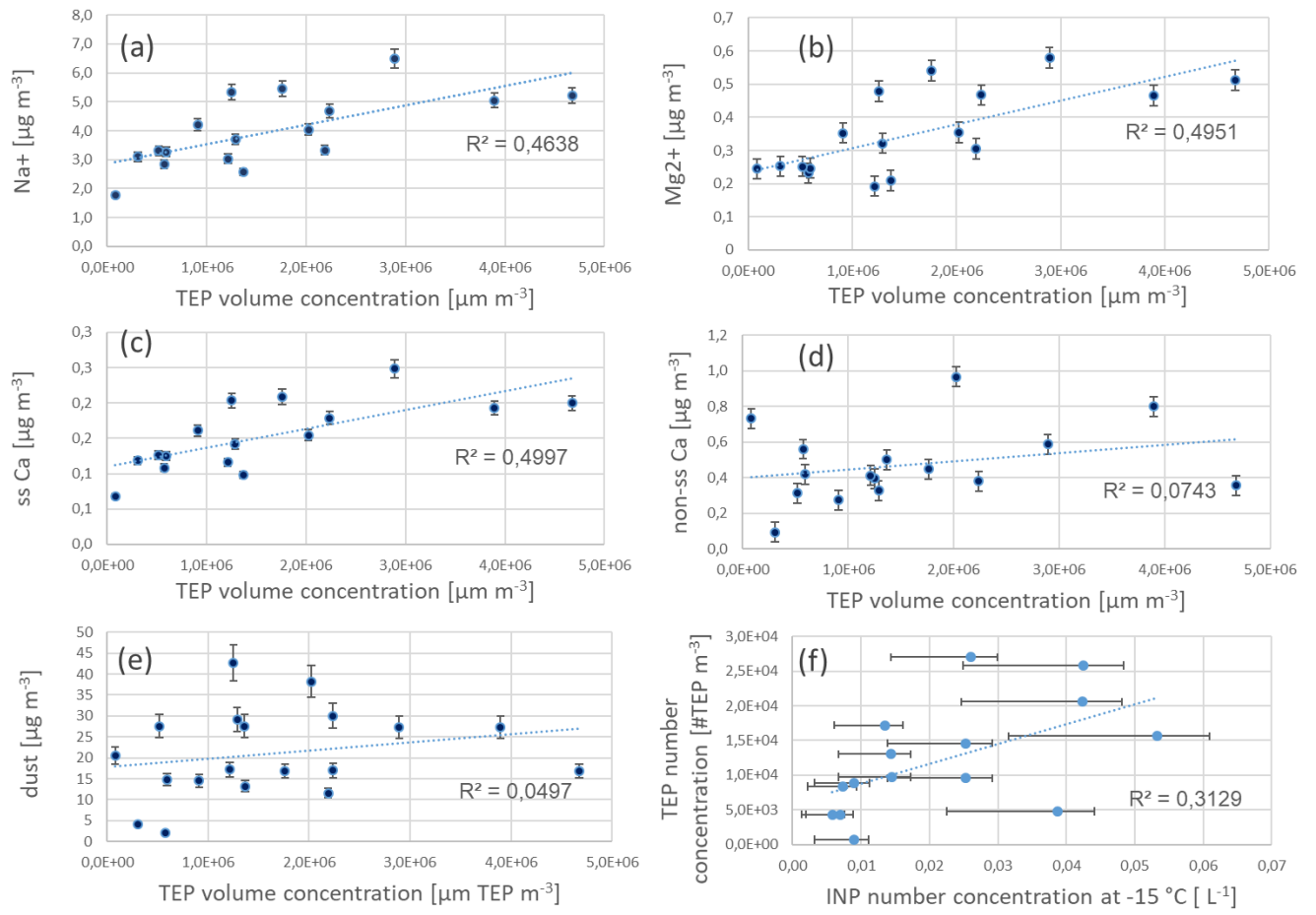
Figure 5

1199
1200
1201



1202
1203
1204
1205
1206
1207
1208
1209
1210
1211
1212
1213

Figure 6



1214

1215

1216

1217

1218

Figure 7